Al-Farabi Kazakh National University

UDC 536.24; 536.71

BERDENOVA BAKYTNUR AMANBAYEVNA

Adsorption Characterization of Composite Activated Carbons for application in Adsorption Cooling Systems

6D060300 Mechanics

Thesis for the degree of Doctor of Philosophy (Ph.D.)

Scientific supervisors:
Kaltayev Aidarkhan
D.Phys.-Math.Sc., Professor

Bidyut Baran Saha
D.Eng., Professor,
Kyushu University,
Fukuoka, Japan

The Republic of Kazakhstan
Almaty, 2020

TABLE OF CONTENTS

ACKNOWLEDGEMENTS

I would like to express my special appreciation and thanks to my local supervisor Prof. Aidarkhan Kaltayev for encouraging my research and for allowing me to grow as a researcher.

I would like to thank my foreign scientific supervisor Prof. Bidyut Baran Saha for letting my defense happen. Thank you for the opportunity to take an internship at your Lab, which was a key point in determining what to do next and where to move. Thanks for all your brilliant comments and suggestions.

I would especially like to thank Dr. Animesh Pal for his help and patience, for me it wouldn't be possible to collect data for investigation for my Ph.D. thesis. I would also like to thank Prof. Kyaw Thu, Dr. Sourav Mitra and all the lab members for making my stay in Japan so enjoyable and cognitive, thank you for your warm welcome and valuable advices.

Special thanks to my family for cheering me up and constant support throughout this experience. I totally appreciate it. Thanks for everything you have done and keep doing for me.

NORMATIVE REFERENCES

In this dissertation, references are made to the following standards:

The Law of the Republic of Kazakhstan “On Science” dated February 18, 2011 №407-IV LRK;

CSSE (GOSO) RK 5.04.034-2011: Compulsory State Standard of Education of the Republic of Kazakhstan, postgraduate education, doctoral candidacy. Main regulations (revised August 23, 2012 №1080).

GOST 7.32-2001 Interstate standard. System of standards on information, librarianship and publishing. The research report. Structure and rules of presentation

GOST 7.1-2003 Bibliographic record. Bibliographic description. General requirements and rules of drafting.

GLOSSARY

Absolute uptake - according to the Gibbs definition, absolute uptake is the amount of gas molecules that are in the adsorbed state in a porous material.

Absorbate – a substance that is adsorbed.

Absorption – the process in which a fluid is dissolved by a liquid or a solid absorbent and involves the entire volume of the absorbing substance.

Activated carbon – a form of carbon processed to have small, low-volume pores that increase the surface area available for adsorption or chemical reactions.

Adsorbent – a substance that adsorbs another.

Adsorption coverage - is fractional coverage of the adsorbent with adsorbate.

Adsorption – the process in which atoms, ions or molecules from a substance (it could be gas, liquid or dissolved solid) adhere to a surface of the adsorbent. Adsorption is a surface-based process where a film of adsorbate is created on the surface.

Consolidated – when powders and granular materials combined together into a unified whole with more pressure so they become stronger or more solid.

Cooling systems – chillers, air conditioners, refrigerators, freezers, ice-making, snow-making machines, engine chillers etc.

Equilibrium/saturation - the condition when the system is in equilibrium, that the chemical potential of the adsorbed molecules is equal to that of the molecules in gas phase, or when the adsorption rate is equal to the desorption rate.

Exothermic process – describes a process or reaction that releases energy through light or heat from the system to its surroundings.

Maximum adsorption capacity - the maximum possible amount of adsorbate that might be taken up by unit mass (or volume) of the adsorbent.

PTW diagram – pressure-temperature-adsorption equilibrium diagram. The PTW diagram is also drawn from the ideal cycle analysis in order to explain the performance of adsorption cooling systems.

Refrigerant – a substance used as a heat carrier in cooling systems.

Working pair – adsorbent-adsorbate pair.

NOMENCLATURE

C_0	saturated amount adsorbed [g g^{-1}]
D_{K_eff}	effective Knudsen diffusivity coefficient [cm^2 s^{-1}]
P_c	critical pressure [kPa]
P_s	saturation pressure [kPa]
R_p	granular adsorbent particle radius [cm]
T_c	critical temperature [K]
T_t	triple point temperature [K]
V_a	adsorbed phase volume [cm^3 g^{-1}]
V_t	molar volume of gas at triple point [$cm^3 g^{-1}$]
W_0	limiting micropore capacity [cm^3 g^{-1}]
c_p	specific heat capacity [$Wg^{-1}K^{-1}$]
k_{th}	thermal conductivity coefficient [$Wcm^{-1}K^{-1}$]
n_{abs}	absolute molar uptake [mmol g^{-1}]
n_{exc}	excess molar uptake [mmol g^{-1}]
q_{abs}	absolute mass uptake [g g^{-1}]
q_{eq}	adsorption equilibrium uptake [g g^{-1}]
q_{exc}	excess mass uptake [g g^{-1}]
q_{in}	initial uptake [g g^{-1}]
z_b	adsorption space thickness [m]
v_{pore}	pore volume [cm^3 g-1]
ΔH_0	isosteric heat of adsorption [J mol^{-1}]
b_0	equilibrium constant [kPa^{-1}]
E	characteristic energy [J mol^{-1}]
k	power, fitting parameter [-]
m	structural heterogeneity parameter [-]
Q	isosteric heat of adsorption [J mol^{-1}]
R	universal gas constant [J mol^{-1} K^{-1}]
t	heterogeneity parameter [-]
t	time [sec]
A	adsorption potential [J mol^{-1}]
C	amount adsorbed [kg kg^{-1}]
M	molar mass of the substance [g mol^{-1}]
P	equilibrium pressure [kPa]
S	specific surface area [m^2 g^{-1}]
T	temperature [K]
W	volumetric adsorption uptake [cm^3 g^{-1}]
$q(t)$	instantaneous uptake [g g^{-1}]
$\bar{q}$	volume averaged adsorption uptake [g g^{-1}]

Greek symbols

α_{th}	thermal diffusivity [cm^2 s^{-1}]
ρ_b	balk gas density [g cm^{-3}]

ρ_{pack} packing or apparent density of the adsorbent [g cm^{-3}]
ρ_{sk} skeletal density [g cm^{-3}]
α thermal expansion of the adsorbed gas [K^{-1}]
ε void fraction, porosity [-]
θ surface coverage, $\theta = C/C_0$
τ tortuosity [-]

Abbreviations

AC	Activated Carbon
ACS	Adsorption Cooling System
ANG	Adsorbed Natural Gas
BET	Brunaure-Emmett-Teller analysis
C-C	Clausius-Clapeyron equation
CFD	Computational Fluid Dynamics
CNG	Compressed Natural Gas
COP	Coefficient of performance
D-A	Dubinin-Astakhov model
GWP	Global Warming Potential
HEC	Binding material, hydroxyethyl cellulose
I2CNER	International Institute for Carbon-Neutral Energy Research
IIR	International Institute of Refrigeration
IUPAC	International Union of Pure and Applied Chemistry
LDF	Linear Driving Force model
MSB	Magnetic Suspension Balance unit
NLDFT	Non-Local Density Functional Theory
ODP	Ozone Depletion Potential
PDEs	Partial Differential Equations
PSD	Pore Size Distribution
PTW	pressure-temperature-equilibrium adsorption uptake
RMSD	Root-mean-square deviation
SCE	Specific Cooling Effect
TGA	Thermal Gravimetric Analysis

ABSTRACT

Relevance of the research topic. According to International Institute of Refrigeration (IIR), approximately 15% of all electricity produced worldwide is used for refrigeration and air conditioning, which means the huge portion of the energy consumed falls to the share of different cooling systems. While using an adsorption process for cooling applications, the electrically powered compressors of conventional compression based systems replaced by thermally driven adsorption bed. This makes ACS fully functional without electricity supply, which allows the use of this technology in remote undeveloped regions. Development of such technology would be useful for Kazakhstan where the towns and villages are very scattered throughout the country. Introduction of the fully solar driven adsorption cooling systems would have a positive socio-economic effect via rational use of energy and its safe operation. The transition to the clean sources of energy would solve different problems with air pollution.

The scientific direction of the research is almost new and developing slowly in Kazakhstan, therefore there are no specialized laboratories equipped with the necessary equipment for developing new types of adsorbents for refrigeration systems, and for analyzing their physical properties. Whereas around the world the given field actively developing. Therefore the research topic is very important and significant on a national scale.

Moreover, the adsorption process is finding application in various fields of science when creating new technologies and techniques. For instances: gas storage, heat pumps, CO_2 capture and sequestration, etc. The growing interest for adsorption process application makes the development of new adsorbent materials and accurate evaluation of their adsorption properties relevant study. Therefore new adsorbents with improved characteristics are being developed and proposed by different authors. An accurate assessment of the adsorption characteristics of newly synthesized materials plays a very important role in determining their thermodynamic properties and forecasting their performance as they used in different systems. Therefore the results of the study also can be used in other adsorption related systems.

Purpose of the study. To determine physical and adsorption properties of the newly synthesized composite activated carbon and develop a scientific basis for the selection of materials for adsorption cooling systems using experimental and numerical methods.

The objectives of the study.

- to conduct experiments to measure the thermal and porous properties of the composite activated carbon;
- to determine adsorption characteristics of carbon dioxide onto the composite material for possible applications in adsorption cooling systems;
- to investigate regularities of isothermal adsorption process using numerical method and determine dynamic characteristics of the process of adsorption.

Object of the research. Composite activated carbon, carbon dioxide adsorption onto consolidated activated carbon, adsorption cooling systems.

Subject of the research. Thermal and adsorption characteristics of composite activated carbon.

Methods. Experimental, mathematical and numerical modeling. Experiments were held at I2CNER Institute in conjunction with the lab members. To analyze the experimental data different regression and other known analytical methods were used. Sample of consolidated activated carbon for study was provided by I2CNER.

The scientific novelty of the study. Provisions to be defended.

- new consolidated composite adsorbent with improved thermal conductivity and volumetric adsorption uptake was synthesized and the adsorption characteristics of the material studied comprehensively. Analysis of the experimental data revealed 233% higher thermal conductivity than that for parent activated carbon;
- excessive adsorption isotherms obtained using thermogravimetric analysis were processed using two different methods for evaluating absolute uptake. In the first method the specific volume of gas in the adsorbed state is assumed to be equal to the specific pore volume. In the other method the volume of adsorbed gas tends to zero under low pressure and/or high temperature conditions. The average was taken as the best closest fit. Obtained absolute adsorption data was fitted to Dubinin-Astakhov and Tóth isotherm models;
- new mathematical model considering the adsorption caused porosity and Knudsen diffusivity changes was developed. The temperature dependent adsorption rate change due to the energy release during adsorption process is also implemented in the model. The effective Knudsen diffusion coefficient for the working pair of CO_2/AC evaluated from Pore Size Distribution data. The experiment conducted on the magnetic suspension balance unit (MSB-GS-100-10 M) to measure the CO_2 adsorption onto consolidated composite activated carbon was simulated.

Validity and reliability. The validity and reliability of the scientific provisions, conclusions and results of the thesis are confirmed by their consistent theoretical and mathematical justification, as well as the obtained simulation results compared with experimental data.

Theoretical and practical significance. Theoretical significance is that the developed mathematical model predicts the adsorption dynamics with better accuracy as it takes into account such factors like porosity and permeability changes with uptake, and adsorption rate changes due to temperature variations as the process of adsorption is exothermic.

The research has a practical significance, because the enhancement of adsorption characteristics of the working pair (refrigerant/adsorbent) in ACS has a positive impact on its performance. Results obtained later will be used in development of the fully solar driven ACS prototype. Such technology could be used in production of from small thermostats till huge storehouses with regulated temperature.

Testing the results of the study. The results obtained on the topic of the work were presented at the following scientific events:

- Report at the city scientific seminar “Mathematical problems of natural sciences. Inverse and incorrect tasks”, Almaty, 2019;
- International scientific conference of students and young scientists “Farabi

alemi”, Almaty, April 8-11, 2019;

- International scientific conference of students and young scientists "Farabi alemi", Almaty, April 10-12, 2018;
- XIII International Scientific Conference of Students, Undergraduates and Young Scientists "Lomonosov-2017", Astana, April 14-15, 2017.

Series of presentations given at the “Fluid mechanics” seminars and the meeting of the department of “Mechanics”.

Assessment of the completeness of the objectives of the study.

All the research objectives are fulfilled. The dissertation is a complete independent research work devoted to the study of the thermal and adsorption characteristics of consolidated activated carbon for use in adsorption cooling systems. The results of the study and the obtained dependence curves are relevant.

Scientific internships. International Institute for Carbon-Neutral Energy Research (I2CNER), Kyushu University, Fukuoka, Japan, June-July 2017.

Publications. The results of the research were discussed and reported at conferences, and published in scientific journals: 3 publications in journals recommended by the *Committee on the Control of Education and Science of the RK* and 1 publication in international peer-reviewed journal *International Journal of Refrigeration* with an impact factor of 3.17 indexed in Scopus DB. The results on the topic of the dissertation were published in the following papers:

Publications in journals:

1) B.Berdenova and A.Kaltayev, “Review of adsorption and thermal characteristics of activated carbon and its application in ANG storage and ACS systems”, Вестник национальной академии наук РК, 2017, №3, P. 27-36.
2) Б.Берденова, Е.Максум, “Регрессионный анализ для определения параметров моделей изотерм адсорбции”, Вестник КазНИТУ, 2018, №4, С. 233-240.
3) B. Berdenova, A. Pal, M. Muttakin, S. Mitra, K. Thu, B.B. Saha, A. Kaltayev, “A comprehensive study to evaluate absolute uptake of carbon dioxide adsorption onto composite adsorbent”, International Journal of Refrigeration, Volume 100, April 2019, P. 131-140, Scopus (IF 3.17), https://doi.org/10.1016/j.ijrefrig.2019.01.014
4) Б.Берденова, “Математическая модель процесса докритической изотермической адсорбции CO2 на активированный уголь”, Вестник КазНИТУ, 2019, №6, С. 751-756.

Abstracts in conference proceedings:

1) Б. Берденова, Стационарные системы адсорбционного охлаждения работающие на экологически чистых хладагентах, XIII Международная научная конференция студентов, магистрантов и молодых ученых «Ломоносов-2017 », г. Астана, 2017, С. 86-87.
2) Ye. Maksum, B. Berdenova, thesis in conference proceeding “Analysis of the thermodynamics of adsorption cooling systems with the working pair of activated carbon/CO2”, “V International Farabi readings”, Almaty, 2018, P. 61.
3) Б. Берденова, Сверхкритический цикл работы холодильного оборудования на углекислом газе, Конференция «Международные Фарабиевские чтения-2019», г. Алматы., 2019, С. 64.

Structure and scope of the Ph.D. thesis. The text of the thesis contains the following elements: abstract, introduction, 5 chapters, conclusion, the reference list of 100 items. The work has been expounded in 70 pages, contains 33 figures and 10 tables. Chapters 2-5 are done in collaboration with the foreign supervisor's group and done as part of a scientific internship to Japan. On collaboration results the joint paper was published.

The introduction of the dissertation provides an overview of adsorption cooling systems, the operation principle of such systems, advantages and disadvantages. It also lists the main methods for increasing the cooling capacity of the material, and ways to make adsorption reactors more compact. The main methods used are the consolidation and enhancement in thermal conductivity of the activated carbon.

The second chapter describes the method and operating principle of an experimental setup for measuring absorption uptake for a working pair of activated carbon/carbon dioxide. Other established intrinsic and adsorption characteristics of the composite material are also listed.

In the third and fourth chapters the methods for estimating the absolute uptake using two different assumptions and correlation of the parameters of the Dubinin-Astakhov and Toss isotherm models are described. In the fifth chapter the isosteric heat of adsorption is studied.

In the sixth chapter, the effective Knudsen diffusion coefficient for a porous medium is obtained using the pore size distribution and the characteristics of the defunding gas.

To calculate the adsorption uptake at the solid-gas interface, and for a detailed description of the dynamics of the adsorption process, a mathematical model of the non-isothermal reactive adsorption was constructed and solved. The mathematical model considers the adsorption caused porosity and Knudsen diffusivity changes. The experiment conducted on the magnetic suspension balance unit (MSB-GS-100-10 M) to measure the CO_2 adsorption onto composite activated carbon was simulated. The result obtained was compared with the results found using non-reactive isothermal model and experimental data. Non-isothermal reactive flow model gives more accurate curve of volume averaged uptake with sharp increase in the adsorption starting and lower rate of mass uptake due to the release of the heat of adsorption. The rate gradually increases with time as the thermal energy dissipates to the surrounding through natural convection. Thus, the dependence curves obtained by this method show better agreement with the experimental results. Residual deviations/errors in the results are associated with the use of 1D model assumption that excludes the gas penetration by the sides of the tablet.

In conclusion, the main results and conclusions of the thesis are presented. Comparison with experimental data shows good measurement accuracy. The results of the presented dissertation are of great theoretical significance, and can be used for a detailed description of the dynamics of adsorption of carbon dioxide in consolidated activated carbon. The main provisions and conclusions of the dissertation are justified.

1 INTRODUCTION

The process of adsorption of gases have been used in various application for instances: gas storage [1-4]; cooling systems [5-9]; energy storage [10-11]; heat pumping [12-13] and CO_2 capture and sequestration [14-16]. For instance, Zakaria and George [2, P. 226] mentioned that during adsorption storage of methane, the pressure in the storage tank is reduced up to 5 times compared to the compression storage. Authors illustrated it regarding the capacity of empty tank and adsorbent filled tank, and showed that the energy density of the adsorbent filled tank is 5 times higher than that of empty tank at 3.5 MPa. Therefore adsorption storage is widely used for utilizing the gaseous fuels like natural gas or hydrogen in vehicles because of its safeness [17]. While using an adsorption process for heating or cooling applications, the electrically powered compressors of conventional compression based systems replaced by thermally driven adsorption bed. Therefore, adsorption cooling/heating systems are fully functional without electricity supply [12, P. 433] which allows the use of this technology in remote regions without access to electricity. The solar energy or the waste heat can be utilized as a source of energy for such systems operation [18-20]. Sumathy and Zhongfu [21] conducted experiments with solar-powered adsorption ice-maker and concluded that AC/methanol pair is one of the most efficient working pair for ice making purposes, for a collector area of 0.92 m^2, it was possible to produce ice of about 4-5 kg/day.

There are two types of cooling systems: adsorption and vapor compression cooling systems. In table 1 illustrated the main pros and cons of each. Working principle of both adsorption and compression cooling systems lies in the use of a refrigerant with a very low boiling point. The main difference between these two systems is the way how the refrigerant is converted from a gas state back to a liquid so that the cycle could repeat. In ACS gaseous refrigerant is absorbed by another material, and the temperature of refrigerant-saturated material increases, which leads to the refrigerants to evaporate out. Hot gaseous evaporated refrigerants pass through a heat exchanger, where they give their thermal energy outside the system and condense. After all, condensed refrigerant go to the initial compartment, where it starts its next cycle. Whereas in compression cooling systems gaseous refrigerant passes through compressor which increases its temperature above surrounding temperature, to assure the refrigerant to give away its thermal energy to the environment.

The performance of ACS depends on selection of working pair and on their thermal and adsorption properties. Depending on the freezing and boiling points of refrigerants, working pairs can be applied for different purposes: refrigeration, ice making, air conditioning, engine chilling etc. Other properties such as latent heat, freezing point and saturation vapor pressure, toxicity, flammability, corrosion etc. also have same importance while selecting the working pair. The common working pairs and their characteristics are illustrated in the table 2. [22] made a review for new pairs for potential cooling applications. Habib et al. [23] mentioned that the system with AC-R134a pair can achieve -10 ^{0}C refrigeration loads.

Table 1 - Comparison of sorption and compression cooling systems

	Advantages	Disadvantages
Adsorption cooling systems (ACS)	a) utilize natural and benign refrigerants such as water, methanol, ethanol, ammonia, CO_2, etc. b) zero global warming potential c) can be driven with solar energy or waste heat which is abundant in summer when the cooling power is the most needed d) can operate off-grid, autonomously e) low operating cost f) simplicity of construction, lack of moving parts g) simple control h) quiet operation, no vibration	a) bulkiness b) higher costs c) low performance
Vapor compression cooling systems	a) compact	a) employs high global warming refrigerants such as R134a (GWP = 1430) for mobile air conditioning and R410a (GWP = 1725) for residential air-conditioning (chlorofluorocarbons (CFCs) or hydrofluorocarbons (HFCs)) b) stresses electric grids in summer c) vibration problems, noise pollution

Table 2 - Working pairs and their characteristics [18, P. 66, 22-24]

Adsorbent	Adsorbate (refrigerant)	Heat of adsorption (kJ/kg)	COP
Silica gel	Water	2800	0.4-0.61
	Methyl alcohol	1000-1500	
Zeolite (various grades)	Water	3300-4200	0.4-0.9
	Carbon dioxide	800-1000	
	Methanol	2300-2600	
	Ammonia	4000-6000	
Activated alumina	Water	3000	
	Ethane	1000-2000	
	Ethanol	1200-1400	
Activated carbon	Methanol	1800-2000	0.12-0.78 [25]
	Water	2300-2600	
	Ammonia	2000-2700	0.61-0.67
	Carbon dioxide	526.6 [26]	
Calcium Chloride	Methanol		

In table 3 illustrated ways of making sorption cooling systems more compact and productive [24, P. 9, 27-28]. The improvement of the thermal conductivity of the adsorbent plays major role [29]. The thermal conductivity is commonly dependent on the apparent density and increases with increasing density. Some examples of such trend can be found in [30].

Table 3 - Ways of overcoming the drawbacks of adsorption cooling systems

Methods	Ways
Presenting new adsorbents	a) specific heat capacity [27, P. 61, 29, P. 695] b) density [27, P. 61, 29, P. 695] c) thermal conductivity [27, P. 61, 29, P 695] d) with higher sorption rate [24, P. 7]
Presenting new refrigerants	
Improving heat transfer coefficients	a) increasing the number of fins in finned tube heat exchangers [29, P. 695] b) optimization of fin spacing and height [24, P. 8] c) consolidating the adsorbent [29, P. 695] d) increasing heat transfer area of adsorber bed i.e., design of new adsorber bed [24, P. 9].

1.1 Operating principle of ACS

Depending on the adsorbent the ACS classified into two main groups: *stationary* and *dynamic*. Adsorption system for each is built differently. In ACS with stationary absorbent only the adsorbate circulates, when in ACS with dynamic adsorbent circulate both. For example, in ammonia/water ACS the water performs the function of an adsorbent, whereas in water/activated carbon pair it is an adsorbate. Activated carbon, silica gel and zeolite are related to solid adsorbents. In case of solid adsorbent the system operates intermittently [31-32]. For example in one-bed solar adsorption refrigeration system the collector is heated during the day and cooled at night. As we see, one-bed adsorption chiller does not chill continuously, but this disadvantage of ACS can be solved by adding few more adsorption beds. Or there exist few types of hybrid adsorption-vapor compression systems in literature [33]. Examples of continuous systems can be found in [34-35]. Through multi-bed operation the COP might be improved.

In figure 1 and figure 2 illustrated the schematics of one-bed adsorption chiller. The operating cycle consists of four main stages:

1. *pre-cooling* of the bed with cooling water leading to the decrease in temperature and pressure in the bed (figure 2, section $C \rightarrow D$);
2. *adsorption* of evaporated gas at constant adsorption pressure, p_a (section $D \rightarrow A$). During this step the heat of adsorption Q_a and cooling Q_c are emitted to the environment. And at point A, at the end of this step, the adsorption bed is saturated with adsorbate;
3. *pre-heating* of the bed with waste heat to increase the temperature and pressure up to condensation pressure (section $A \rightarrow B$);
4. *desorption* during which adsorbent is removed from the bed and flows into the condenser, where it gives some energy Q_{cond} to the surrounding, condenses and flows into the reservoir (section $B \rightarrow C$). During this step the heat of desorption Q_d and waste heat Q_h are taken by the adsorption bed. At point C the adsorbent bed is fully regenerated and cycle repeats.

For ACS the Coefficient of performance (COP) is calculated as the ratio of the heat extracted by the refrigerant evaporation Q_e (cooling energy) to the waste heat amount Q_h received by the adsorption bed. In solar ACS, Q_h is the solar irradiation received by the area of the collector. For example, in [7, P. 2000] the cooling performance of solar powered adsorption refrigerator (with an activated carbon/methanol working pair) was tested during 14 days. During this period the daily mean ambient temperature varied between 14-18 ^{0}C. Depending on the weather the irradiation received by the collector varied from 12 000 to 27 000 kJ/m^2. The temperature achieved in the cooling box by the evaporation varied between 8.1 ^{0}C and -5.6 ^{0}C. Thereby the COP of the refrigeration unit is found 5-8%.

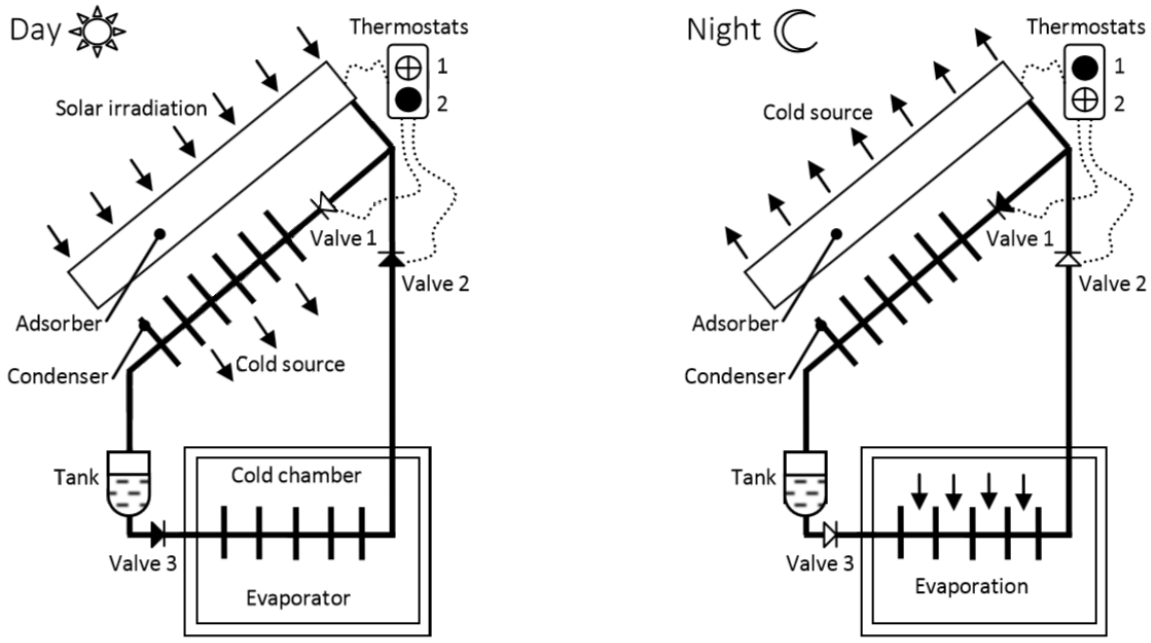

Figure 1 - Main compartments of simple solar adsorption refrigeration system [36]

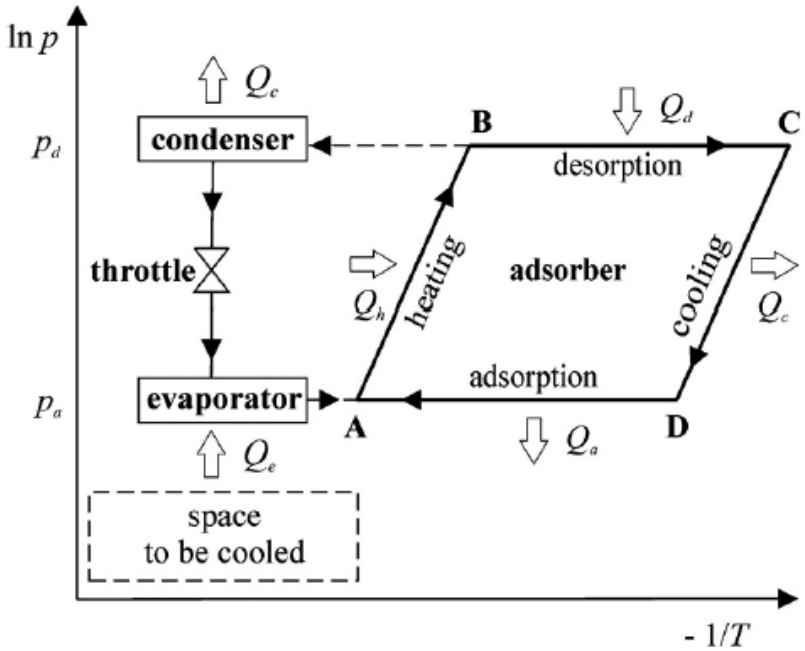

Figure 2 - Thermodynamic analysis of ACS: the ideal cycle in the Clapeyron diagram [18, P. 64]

1.2 Carbon dioxide as a refrigerant

The carbon dioxide is the promising refrigerant because it provides numerous benefits including high volumetric capacity and availability. Furthermore, it is a nonflammable, non-toxic refrigerant having zero ODP and GWP (= 1) [8, P. 304].

Depending on the refrigerant's phase transition the working cycle might be subcritical or supercritical. Carbon dioxide reaches its critical point at 31 °C, 7.38

MPa. When developing refrigerator with the required temperature in the outlet, it is also necessary to take into account the triple point, −56.6 °C, 0.52 MPa, at which three phases exist in equilibrium. At lower temperatures dry ice may form and CO_2 circulation cycle becomes impossible. The condensation is not possible at temperatures above 31°C. In the subcritical cycle, the range of operating temperatures and pressures is between the triple and critical points. If the working range of pressure and temperature goes beyond the critical point, then such a cycle is called super or trans critical. The required cooling load, the ambient temperature, as well as the radiation intensity, establish key points on the working cycle diagram of the refrigeration equipment. Carbon dioxide is a high pressure circuit refrigerant. For thermodynamic analysis of working pairs the PTW diagrams are used. It shows the relation among pressure, temperature and adsorption uptake.

1.3 Current state

The theory of adsorption includes many gross assumptions and corrections. Adsorption uptake is one of the key parameter and fundamental characteristics to determine the performance of ACS. However, there is no equipment that measures directly absolute adsorption of CO_2 and also other high pressure gasses such as CH_4, R32 and N_2 [37]. Since CO_2 is a high pressure gas, the evaluating of absolute uptake is a vital problem in the field of adsorption. During the adsorption process, pore volume is partially occupied by the adsorbate molecules in the solid state and partially with molecules in free molecular phase. According to the Gibbs definition, absolute uptake is the amount of gas molecules that are in the adsorbed state in a porous material. Sometimes all the adsorbate molecules entering through the envelope of the adsorbent particles is considered as absolute uptake, no matter is the molecule in the adsorbed or free gas state. The precise definition of absolute adsorption uptake from excess adsorption is a critical problem since it requires knowing either the density or the specific volume of adsorbed gas, which is very difficult to determine and they are functions of temperature and pressure. The theory behind to evaluate absolute uptake includes many assumptions which are [38, P. 241]:

1. Assuming the density of the adsorbed phase is equal to the density of the saturated liquid.
2. Regarding the adsorbed phase as closely packed molecules at a specified diameter, usually corresponding to the van der Waals volume.
3. Evaluating the adsorbed phase density based on the linear section of the excess adsorption versus bulk density plot.
4. Assuming the volume of the adsorbed phase is equal to that of pores.

Shen et al. [37, P. 399] measured the adsorption of CO_2 onto activated carbon (AC) beads employing gravimetric method. To obtain the absolute adsorption, authors corrected the measured excess adsorption using the above mentioned assumption one. Jribi et al. [39] investigated the adsorption isotherms and kinetics of CO_2 onto AC powder of type Maxsorb III using gravimetric method. To obtain the absolute adsorption, the measured excess adsorption data are corrected using the above

mentioned assumption four. Processing of experimental results differs depending on the technique used for the adsorption measurement: volumetric or gravimetric [40-41].

Recently, scientists are working on how to make ACS more compact and efficient by development of composite adsorbent material with enhanced thermal conductivity and volumetric uptake [42-45]. Wang et al. [45, P. 2066] demonstrated how the consolidation of granular AC helps to improve the thermal conductivity. Authors improved the value by about ten times compared with granular carbon. Jin et al. [43, P. 681] presented the comparison of thermal conductivity and permeability of three different types of AC: granular, consolidated with chemical binder (AC/CB) and consolidated with expanded natural graphite (AC/ENG). The granular and AC/CB adsorbents have better permeability performance than AC/ENG adsorbent, though the thermal conductivity of AC/ENG sample could reach 2.61 $W \cdot m^{-1} \cdot K^{-1}$ which is six times higher than that for other two samples.

In this study, we synthesize consolidated composite adsorbent with a composition ratio of 50 wt% activated carbon (Maxsorb III), 40 wt% graphene, 10 wt% HEC for enhancing the thermal conductivity as well as volumetric adsorption uptake. Porous properties and thermal conductivity of synthesized composite are investigated. In addition, adsorption characteristics of CO_2 onto composites are observed for adsorption temperature of 20 to 70°C up to 5 MPa thermogravimetrically using magnetic suspension adsorption measurement apparatus. The present work also discusses comprehensive study for evaluating accurate absolute adsorption uptake. Obtained absolute adsorption data were fitted to modified D-A and Tóth isotherm models to find the isotherm parameters and heat of adsorption.

There are numerous mathematical models for fixed-bed adsorption of carbon dioxide in literature. Jribi et al. [39, P. 1944], Rashidi et al. [46], Balsamo et al. [47] and Ahn et al. [48] investigated adsorption kinetics of CO_2 onto different sorts of activated carbon and carbon based monolith. Some system configurations allow describing the adsorption dynamics using only LDF mass transfer rate model. It works well for granular AC as the adsorption occurs almost uniformly in the pellets thanks to the presence of voids between particles. For the cases of large industrial units the LDF model is solved in pair with the mass balance equation for mobile gas phase [49]. Usually the void fraction available for the gas phase assumed to be constant. The process of absorption is accompanied by the heat release and the system is never in thermal equilibrium. Some studies neglect the heat of adsorption effect for slow processes, particularly for the cases of gas adsorption when there are no sudden and frequent change in pressure and temperature for hours or so, and use isothermal model which is reasonable and simplifies the calculation procedure. There are works where the adsorption heat effects studied using non-isothermal dynamic simulation in a fixed bed [50-53].

Mathematical models for adsorption onto consolidated and granular activated carbon differ. Present research proposes a mathematical model, non-isothermal reactive flow model, for adsorption onto consolidated material. The model considers

porosity change available for mobile gas and change in Knudsen diffusivity coefficient with adsorption uptake. These effects becomes important when deal with consolidated AC, as in case of consolidated AC the shell of the material saturates first and becomes less permeable for bulk gas. Therefore to find critical thickness for the tablets for application in different adsorption based systems these effects should be taken into account. The system of PDEs was solved in Python using an explicit finite difference scheme. The effective Knudsen diffusion coefficient for the working pair of CO_2/AC evaluated from Pore Size Distribution data. The behavior of curves tested using 1D axial dispersed plug flow geometry. A comparative analysis of the existing and developed mathematical models with the experimental data is done. The developed mathematical model predicts the adsorption dynamics with better accuracy for the given configuration.

2 EXPERIMENTS

2.1 Synthesis of composite

In this study, we synthesized consolidated activated carbon (Maxsorb III) composite adsorbent using graphene nanoplatelets (C750) and hydroxyl cellulose (HEC) as a binder. The composition ratios were 50 wt% Maxsorb III, 40 wt% C750, and 10 wt% HEC for enhancing the thermal conductivity as well as volumetric adsorption uptake. The synthesized procedure can be explained as follows [54-56]. At first, Maxsorb III and C750 were dried in an oven at 150°C for several hours to remove the moisture content and minimize the weight measurement error. The binder HEC is a granular type. To make the HEC solution, water was added into the binder. After that Maxsorb III and C750 were mixed and put them into the binder solution. The mixer was compressed using a mechanical compressor. Finally, the composite sample was dried in the oven at 120°C for several hours to remove the water content. After that, the same composite is used for characterization such as porous properties, thermal conductivity, and CO_2 adsorption characteristics. The photograph and physical properties of the synthesized composite are presented in figure 3.

2.2 Characteristics results of composite

BET surface area. Nitrogen (N_2) adsorption onto the adsorbent is one of the standard methods to determine the porous properties such as specific surface area, pore volume and pore size distribution of adsorbent material [44, P. 136, 57-58]. The N_2 adsorption/desorption isotherm of the synthesized composite was investigated using the volumetric method employing 3Flex™ Surface Characterization Analyzer supplied by Micromeritics, Japan. In this experiment, a pressure transducers accuracy of 0.15% of the reading with a resolution to 10^{-5} mmHg is employed to measure the pressure of N_2 adsorption gas. The measurement error range is automatically calculated by the analyzing software given by 3Flex manufacturer and always shown in BET surface area value. N_2 adsorption/desorption experiment was conducted at −196 °C (77 K) after a regeneration temperature at 250 °C for several hours. Figure 3 shows the N_2 adsorption/desorption isotherm onto studied composite. It can be seen that there is no hysteresis which is essential for adsorption heat pump applications. A characteristic of this figure represent that composite is mostly microporous. Brunaure-Emmett-Teller (BET) method with multi-point surface area analysis was adopted to calculate the surface area. It is found that composite possesses the BET surface area about 1778 ± 13 m^2 g^{-1}.

Pore-size distribution. The PSD analyses were carried out using the Non-Local Density Functional Theory (NLDFT) by applying the provided software package of 3Flex. Figure 4 shows the cumulated pore volume and PSD analysis of the composite adsorbent. It is observed that the total pore volume of composite is 1.014 cm^3 g^{-1}. The surface area and pore volume of the present study along with published various carbon based adsorbents are also enlisted in table 7.

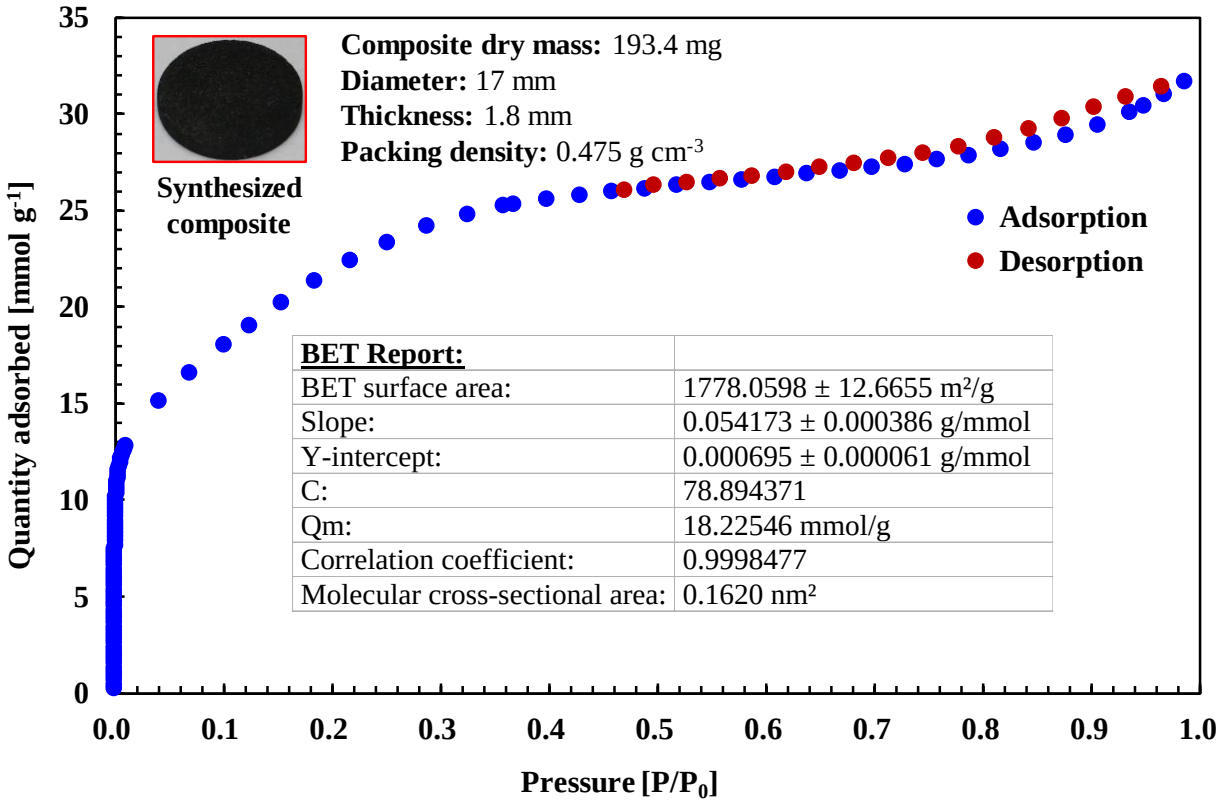

Figure 3 - N_2 adsorption and desorption isotherm onto composite

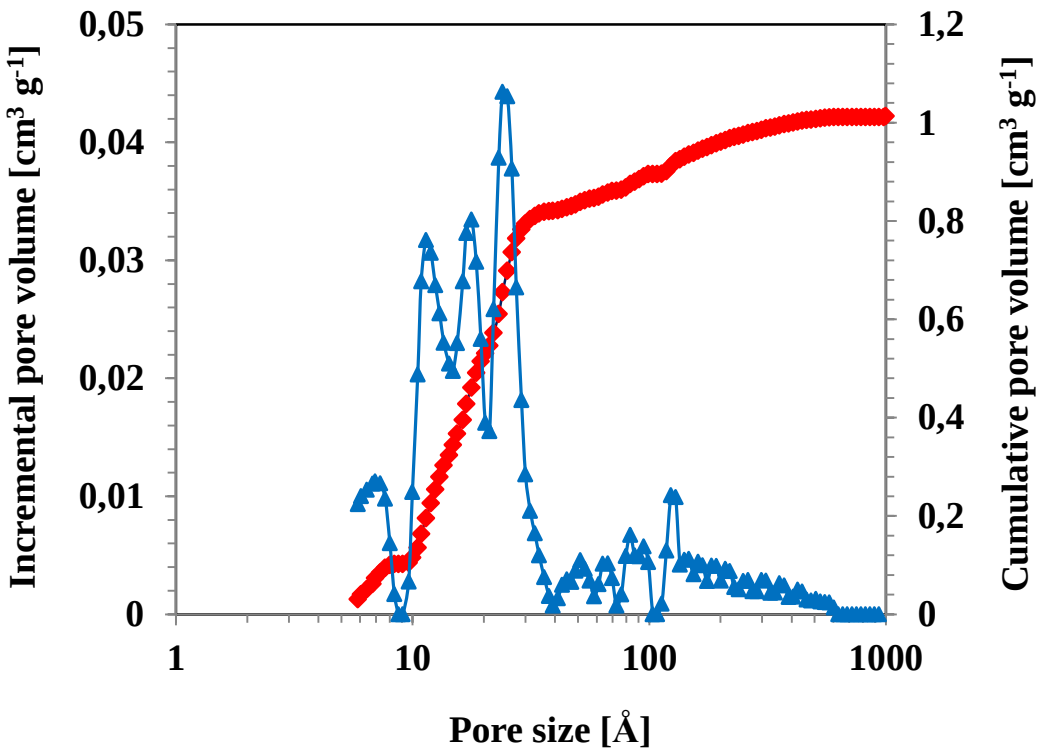

Figure 4 - Pore size distribution analysis of composite

Thermal conductivity. The thermal conductivity of the synthesized composite adsorbent was measured using The NETZSCH LFA 457 MicroFlash system. The details of instrument and measurement procedure of thermal conductivity can be found elsewhere [42, P. 1218]. The thermal diffusivity can be measured by this instrument with an accuracy and repeatability of ±3% and ±2%, respectively. The composite thickness was 1.8 mm measured by using QuantuMike micrometer with resolution of 0.001 mm and instrumental error of ±1μm. The measurements were conducted at room temperature and atmospheric pressure conditions. The thermal diffusivity of each sample was measured six times, and the standard deviation for the measured data was calculated and found ±0.01 standard deviation. The studied composite possesses thermal diffusivity and thermal conductivity 0.564 ± 0.01 mm^2 s^{-1} and 0.22 W m^{-1} K^{-1}, respectively. It should be noted that composite shows 233% higher thermal conductivity compared to parent adsorbent.

Rocky et al. [59] experimentally investigated the specific heat capacity of consolidated composite adsorbents for other mass fractions of Maxsorb III and thermal conductivity enhancers such as expanded graphites and graphene nanoplatelets.

2.3 Adsorption uptake measurement

The magnetic suspension balance unit (MSB-GS-100-10M) supplied by BEL Japan was used to measure the adsorption isotherms of CO_2 onto composite. Figure 5 shows the pictorial view of instrument. A detailed description of this instrument can be found in reference [8, P. 306, 39, P. 1942]. Briefly, it consists of magnetic suspension balance unit; an evaporator; isothermal circulation oil bath to control the adsorption/evaporation temperatures; isothermal air bath to avoid condensation within the system; and a series of vacuum pumps including rotary, diaphragm and turbo-molecular pump. One absolute pressure gauge 10000 kPa, Keller PAA-35X is used to measure the pressure of CO_2 gas with an uncertainty of ±0.1 of full scale. The system contains a platinum temperature element (Pt 100Ω) to control and measure the temperature of the sample section. It is connected to the Julabo (type: F25-ME) circulation oil bath and measurable temperature range is –100 to 250°C.

Measurement procedure can be described as follows; Firstly, the consolidated composite adsorbent of amount 193.4 mg was put into the sample container and connected to the measuring unit of the system. After that, we performed the leak test. The sample was then heated at 130°C for several hours under vacuum condition for each isotherm to remove any adsorbed gas. After that, the temperature was stabilized for measurement condition. Measurements were conducted at six different adsorption temperatures ranging from 20 to 70°C with pressure up to 5 MPa for each temperature: two isotherms from subcritical and four isotherms from supercritical regions. The whole experiment is executed automatically by the instruction given in software. The sample weight is directly measured by magnetic suspension balance with ±1μg resolution. Mass measurement repeatability of magnetic balance is ±30 μg with relative error of ±0.002% of the reading. Since the composite mass used in the

study was about 193.4 mg, so the relative experimental error was always less than 0.002%.

Figure 5 - High Pressure Gas Adsorption Facility MSB-GS-100-10M

3 ABSOLUTE ADSORPTION UPTAKE ESTIMATION

In figure 6 the solid line shows the dependency of adsorbate density on the distance from the surface [38, P. 221]. During adsorption, the density of adsorbate molecules has higher value within the small distance from the solid surface because gas molecules at adsorbed phase are packed densely. The thickness of the adsorption space, z_b, depends on the number of adsorbate layers. In adsorption space, the density of gas equal to the bulk density, ρ_b. So, assuming uniform adsorption and by treating the 3D solid-gas interface as an imaginary mathematical surface then the absolute adsorption, is found as follows:

$$q_{abs} = S \int_0^{z_b} \rho(z) dz \tag{1}$$

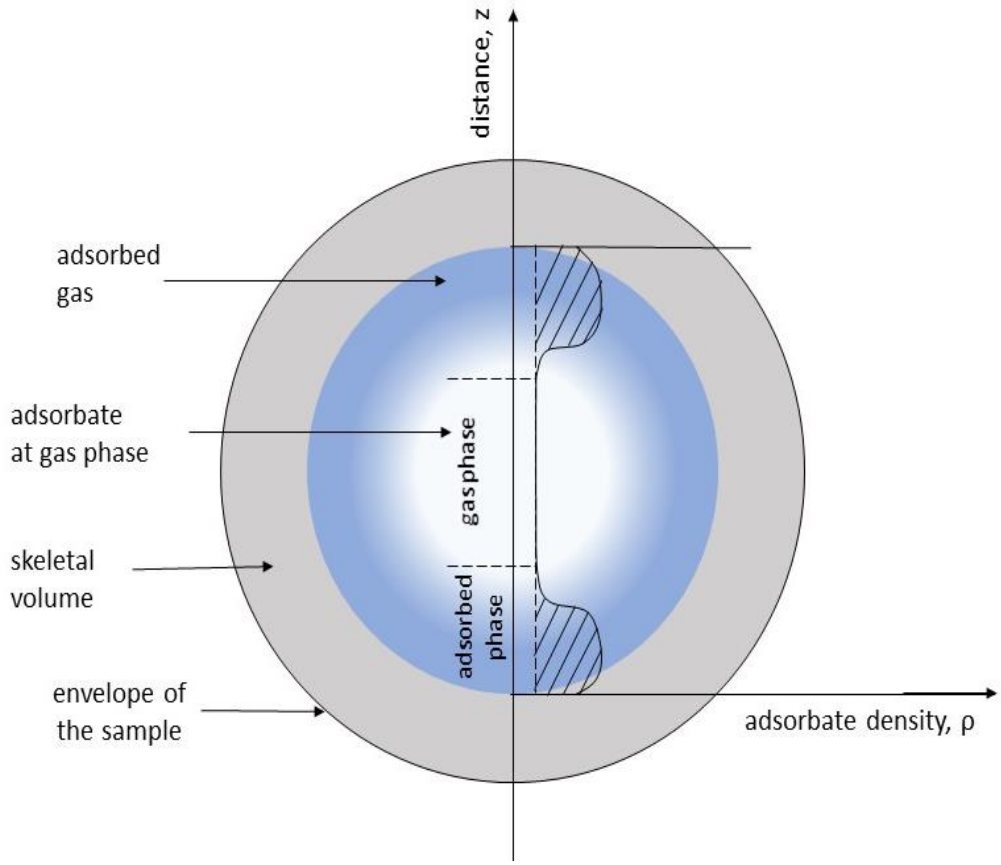

Figure 6 - Schematic illustration of adsorption process. Dependency of adsorbate density on the distance from the solid surface

The experimental data measured by gravimetric apparatus (TGA) gives lower value of adsorption uptake than the value really enclosed in the adsorbent sample, because the sample is weighted while immersed in a bulk gas, and pushed up by Archimedes' force equal to the weight of gas displaced by the skeletal volume of the adsorbent sample and adsorbed phase volumes. Therefore, corrections for both the skeletal volume of the sample and the volume of the adsorbed phase must be done in order to find the correct absolute adsorption values. The TGA apparatus does the

buoyancy correction for skeletal volume before providing the data; therefore, it gives excess adsorption. The excess adsorption corresponds to the shaded area in figure 6, and evaluated as:

$$q_{excess} = S \int_0^{\infty} (\rho(z) - \rho_b)\, dz \tag{2}$$

or

$$q_{excess} = S \int_0^{z_b} (\rho(z) - \rho_b)\, dz \tag{3}$$

As for $z \geq z_b$ the gas density $\rho\ (z) = \rho_b$. Therefore, the absolute adsorption can be found by adding the product of the balk density and the adsorbed phase volume to the value of excess adsorption. The absolute adsorption here is the number of moles of gas contained in all the accessible pore volume of the porous material. The adsorbed phase volume, V_a, is the product of the adsorption space thickness, z_b, by the specific surface area, S.

$$q_{abs} = q_{excess} + \rho_b \cdot V_a \tag{4}$$

$$V_a = S \cdot z_b \tag{5}$$

At supercritical regimes, the volume of the adsorbed phase V_a becomes negligible because the strength of gas-gas interaction is too weak that only single layer adsorption is possible on the wall. That is why excess adsorption and absolute adsorption in supercritical regimes do not deviate much as in sub-critical regimes.

In this study two methods for the evaluation of the absolute uptake are considered: a) the specific volume of gas in the adsorbed state is equal to the specific pore volume [8, P. 304-311]; b) assuming that the absolute uptake is equal to excess uptake, or V_a is almost zero under low pressure and/or high temperature conditions [60-62]. The details of these methods are explanied in the following sections. The values of equilibrium bulk gas density at different temperatures and pressures are taken from NIST Standard Reference Database (REFPROP v9.0).

3.1 Absolute adsorption estimation using the first method

According to the first method, $V_a = V_{pore}$, the absolute adsorption can be found from excess adsorption using the following equation.

$$q_{abs} = q_{excess} + \rho_{CO_2} \cdot V_{pore} \tag{6}$$

3.2 Absolute adsorption estimation using the second method

According to the second method, firstly the experimental excess uptake data are constructed in terms of ln (P/n) versus n excess adsorption, which is called the virial form of the adsorption data and illustrated in figure 7.

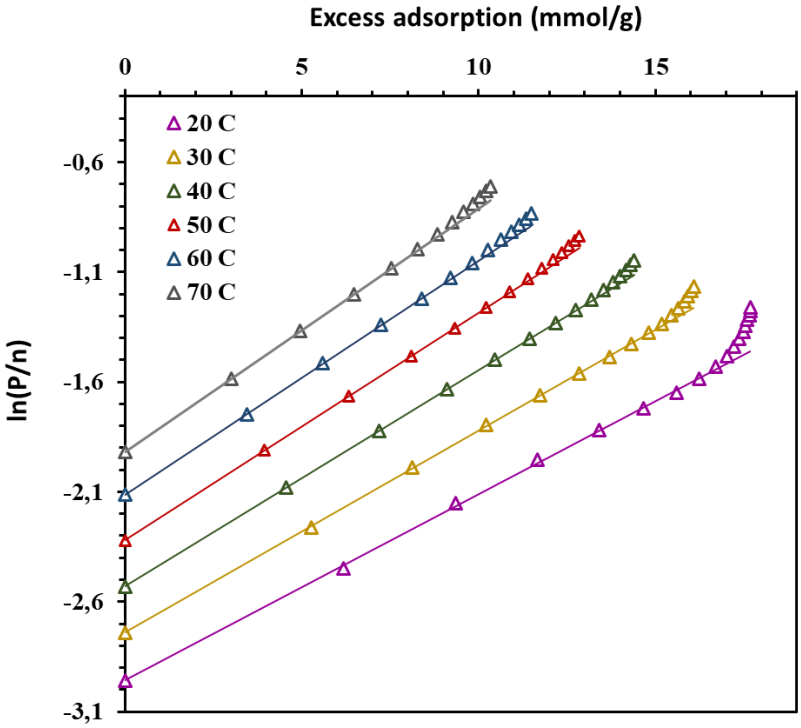

Figure 7 - Virial plot of adsorption data

The curves have a linear form at low surface concentrations, which is used in the evaluation of Henry constants *K(T)*. The obtained values of Henry constants for different temperatures are given in table 4.

Table 4 - Evaluated Henry constants

Temperature [K]	Intercept	K	ln K
293.15	-2.956	19.22093405	2.956
303.15	-2.7402	15.4900828	2.7402
313.15	-2.5317	12.57486525	2.5317
323.15	-2.3199	10.17465679	2.3199
333.15	-2.1131	8.273850506	2.1131
343.15	-1.9172	6.801886499	1.9172

The plot of Henry constants versus temperature in terms of ln (K) versus $1/T$ is known as *van't Hoff plot*, and for the adsorbent-adsorbate pair under the consideration it shows linear dependency. By this means the Henry constants can be derived as a function of temperature. The best-fit straight line with an accuracy value of approximation $R^2 = 0.9989$ is as following:

$$K = \exp\left(-4.1703 + \frac{2093.7}{T}\right) \tag{7}$$

$$K = K_0 \exp\left(-\frac{\Delta H_0}{RT}\right) \tag{8}$$

The advantage of the second method is that it allows the evaluation of the isosteric heat of adsorption (enthalpy or also referred to as limiting heat of adsorption) at this stage, using Eq. 9. From the log-log plot of K versus $1/T$ the isosteric heat of adsorption is found to be $\Delta H_0 = -17.407$ kJ mol^{-1} and K_0 =0.0154.

$$\frac{d \ln K}{dT} = \frac{\Delta H_0}{RT^2} \qquad \text{or} \qquad \frac{d \ln K}{d\left(\frac{1}{T}\right)} = -\frac{\Delta H_0}{R} \tag{9}$$

Let, $K{\cdot}p$ be the product of the Henry constant by the pressure. Figure 8 illustrates the comprehensive adsorption curve in terms of ln ($K{\cdot}p$) versus ln (n), where all isotherms reduce into a single generalized linear line. Linear section of the comprehensive adsorption curve corresponds to the low surface coverage.

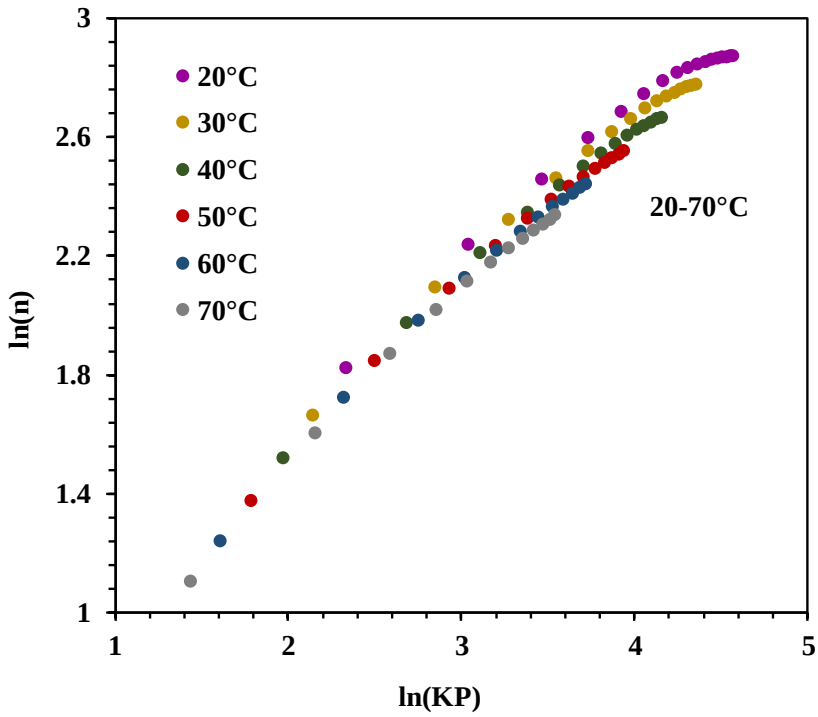

Figure 8 - Comprehensive adsorption curve

Data points corresponding to low surface concentrations are used for estimation of absolute uptake. Second linearization transformation is done by the representation of adsorption isotherms in ln (ln n) versus 1/ln p coordinates as shown in figure 9, from where the values of slope (β) and intercept (α) of each line found and used in construction of generalized absolute adsorption model. Obtained values of α and β are given in table 5.

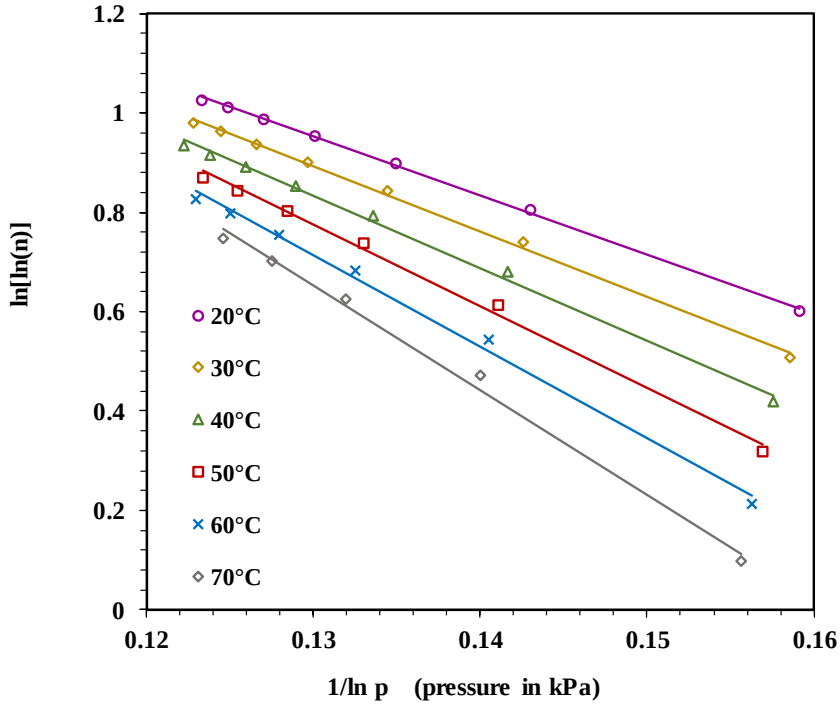

Figure 9 - Second linearized transformation of adsorption isotherms

Table 5 - Values of α and β at different temperatures

Temperature [K]	α	β
293.15	2.4952	-11.868
303.15	2.6039	-13.157
313.15	2.7237	-14.543
323.15	2.9133	-16.446
333.15	3.1048	-18.393
343.15	3.3953	-21.086

By this means, values of α and β can be found as a function of temperature, Eqs. 10-11 (figure 10).

$$\alpha(T) = 0.0177 * T - 2.7566 \tag{10}$$

$$\beta(T) = -0.182 * T + 41.989 \tag{11}$$

As a result, the generalized absolute adsorption model according to the second method is described by the Eqs. 12-13.

$$\ln[\ln n] = \alpha(T) + \frac{\beta(T)}{\ln p} \tag{12}$$

or

$$n_{abs} = \exp\left[\exp\left(\alpha(T) + \frac{\beta(T)}{\ln p}\right)\right] \tag{13}$$

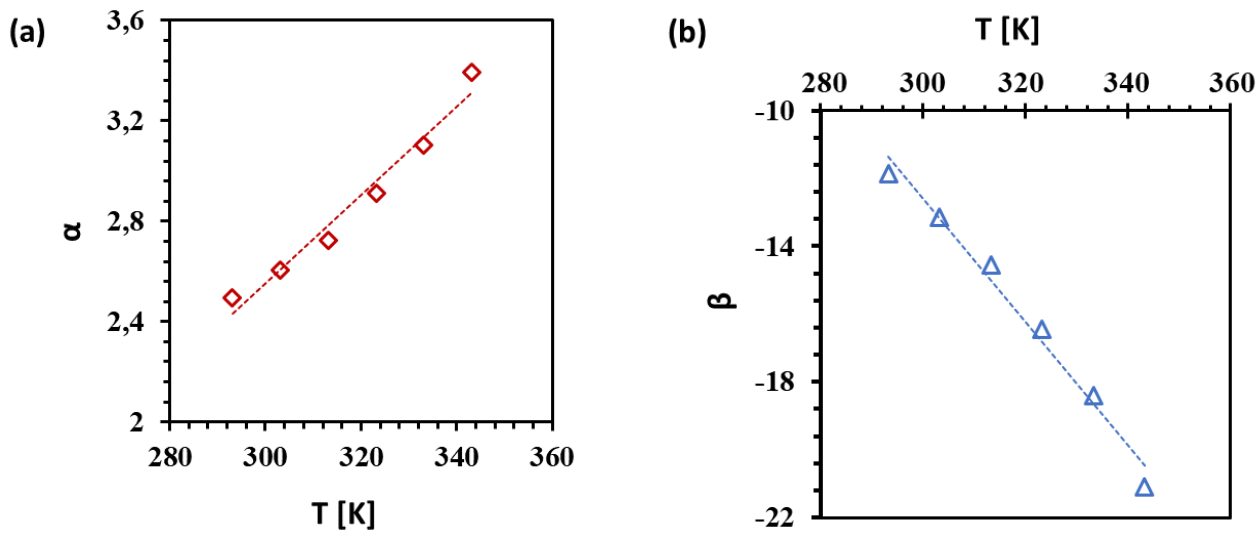

Figure 10 - (a) α and (b) β as functions of temperature

Absolute adsorption values calculated using the methods discussed in sections 3.1-3.2 illustrated in figure 11. To unload the figure, only 20°C and 70°C isotherms are shown. As can be seen from figure 11, while using the first method the absolute uptake always exceeds experimental excess adsorption, whereas in the second method absolute and excessive adsorption data overlap at lower pressure values. As the first method assumes the adsorbed phase volume is equal to the pore volume, $V_a = V_{pore}$, which means that the case considers all the adsorbate molecules entering through the envelope of the adsorbent sample (through the shell of the sample) as an absolute uptake, this assumption gives higher value for volumetric uptake. However, in the second method considers as an absolute uptake only the amount of molecules that are in the adsorbed state in the sample. Therefore, the molecules in the pore volume, which are in the free gas phase (not in the adsorbed state), are not taken into account. This is implemented through the assumption that under high pressure and/or temperature conditions the adsorbed phase volume is almost zero, $V_a = 0$ (when $P \rightarrow 0$ and/or $T \rightarrow \infty$). Therefore, the excess uptake can be considered as absolute uptake and the curves are overlapped at this region.

3.3 Proposed method: averaging the two methods

Above mentioned two absolute uptake estimation methods can be referred as two extreme assumptions, and allow knowing the upper and lower limits of possible absolute adsorption value. Ideally the absolute adsorption is found by adding to the excess uptake the mass of balk gas contained in the adsorbed phase volume, V_a, (Eq. 4). The true absolute adsorption value is somewhere in-between the data obtained using both methods, therefore the average should give the best closest fit (Eq. 14) [63].

$$q_{abs}^{ave} = \frac{q_{abs}^{I} + q_{abs}^{II}}{2} \tag{14}$$

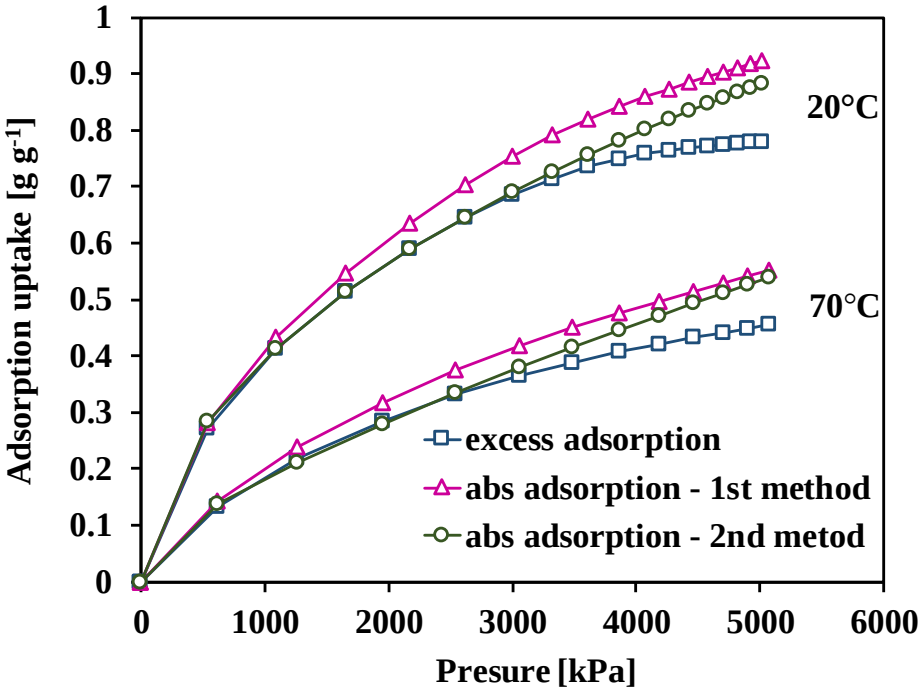

Figure 11 - Experimental excess uptake versus absolute uptake estimated according to the first and second methods

4 ADSORPTION ISOTHERM MODELS

Foo and Hameed [64] made a comprehensive review about existing isotherm models in literature and modeling of adsorption isotherm. International Union of Pure and Applied Chemistry (IUPAC) classified adsorption isotherms into eight main types for different "adsorbent-adsorbate" pairs [65]. The carbon based composite/CO_2 pair falls into the Type-I(b) isotherm. Most used models for this isotherm type are Toth and D-A.

Absolute adsorption data obtained by application of two main methods and the average of them were fitted to modified D-A and Tóth models. Modified Dubinin-Astakhov model can be expressed as (Eq. 15-18) [8, P. 306-308, 39, P. 1943].

$$q_{abs} = \frac{W_0}{V_m} \exp\left(-\left(\frac{A}{E}\right)^m\right) \tag{15}$$

Where,

$$A = RT \ln\left(\frac{P_s}{P}\right) \tag{16}$$

$$P_s = \left(\frac{T}{T_c}\right)^k P_c \tag{17}$$

$$V_m = V_t \exp(\alpha(T - T_t)) \tag{18}$$

Where, W_0 is the limiting micropore volume [cm^3 g^{-1}], A is the adsorption potential [J mol^{-1}], E characteristic energy [J mol^{-1}], m structural heterogeneity parameter [-], V_m is the molar volume of adsorbed phase [cm^3 g^{-1}]; T_c critical temperature [K], P_c critical pressure [kPa], T_t triple point temperature [K], V_t molar volume of liquid carbon dioxide at triple point which is 0.84858 cm^3 g^{-1}; α is the thermal expansion which is 0.0025 K^{-1} [8, P. 307]. k is exponent for calculating the saturation pressure above critical temperature. If k = 2, then the Eq. 15 is called classical D-A model [66], otherwise it is called modified D-A model.

Tóth model is expressed by Eq. 19.

$$\frac{C}{C_0} = \frac{b_0 e^{\frac{Q}{RT}} P}{\left(1 + \left(b_0 e^{\frac{Q}{RT}} P\right)^t\right)^{1/t}} \tag{19}$$

Where C is the amount adsorbed [g g^{-1}], C_0 is the saturated amount adsorbed [g g^{-1}], Q is the isosteric heat of adsorption [J mol^{-1}], b_0 is the equilibrium constant [kPa^{-1}], P is the equilibrium pressure [kPa]. Root-mean-square deviation (RMSD) is used as a measure of prediction error, Eq. 20.

$$RMSD = \sqrt{\frac{\sum_{i=1}^{n}(\hat{y}_i - y_i)^2}{n}} \quad (20)$$

Figure 12-13 represent the graphical illustration of the results of fitting absolute adsorption data obtained by two main methods with modified D-A and Tóth models. It is observed that both isotherm models are fitted well with absolute uptake calculated using both methods. However, Tóth model is better for 1st interpretation whereas modified D-A is better for 2nd interpretation. Averaged Tóth model shows low RSMD value compared to averaged modified D-A model. Isotherm parameters and RMSD of both models are shown in table 6. The maximum uptake of composite/CO_2 pair is found to be 1.02 cm^3 g^{-1} and 2.71 g g^{-1} for modified D-A and Tóth model, respectively. The power *k*, from modified D-A model, for setting pseudo vapor saturation pressure [67], is comparable with the one obtained for CO_2 adsorption onto another AC studied in [39, P. 1944], where the value was found to be k = 4.504. Graphical comparison of all three methods is illustrated in figure 14 (a) and (b) in terms of modified D-A and Tóth model, respectively. The maximum adsorption uptake of CO_2 onto various conventional carbon based adsorbents reported in literature is presented in table 7 and compared with present study. In [68] presented the results of fitting to the Langmuir isotherm additionally.

Table 6 - Parameters for global modified D-A and Tóth isotherm model fitted to the absolute adsorption evaluated according to the first and second method and by averaging method

Estimated parameters	1st method	2nd method	Averaging method
Modified D-A Model			
k [-]	4.56441	4.14575	4.365462
E [J mol^{-1}]	5068.48	4703.68	4900.28
m [-]	1.141005	1.06136	1.103914
W_0 [cm^3 g^{-1}]	1.02570	1.00814	1.01487
RMSD [%]	0.791	0.751	0.621682
Tóth Model			
C_0 [g g^{-1}]	2.714573	2.548024	2.630838
b_0 [kPa^{-1}]	1.88922E-07	1.8892E-07	1.8892E-07
Q [J mol^{-1}]	19025.94	19021.25	19023.58
t [-]	0.477183	0.477179	0.477317
RMSD [%]	0.366	1.0647	0.5644

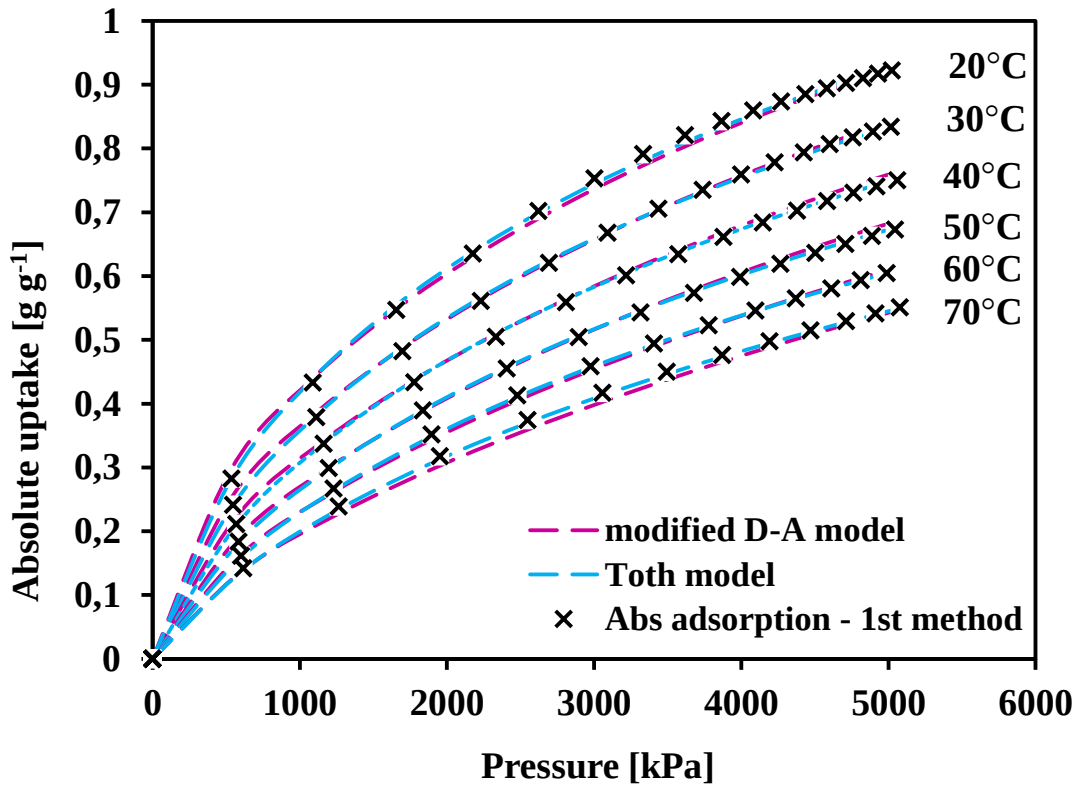

Figure 12 - Modified D-A and Tóth isotherm models fitted with the absolute adsorption estimated using the first method

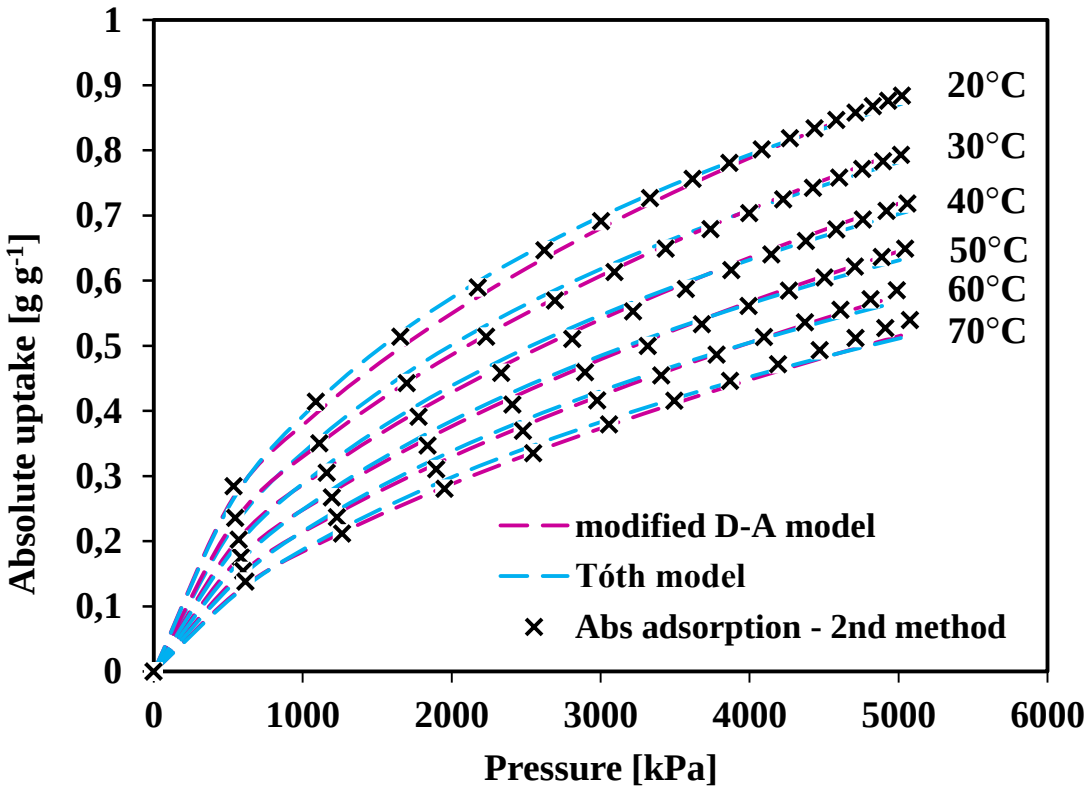

Figure 13 - Modified D-A and Tóth isotherm models fitted with the absolute adsorption estimated using the second method

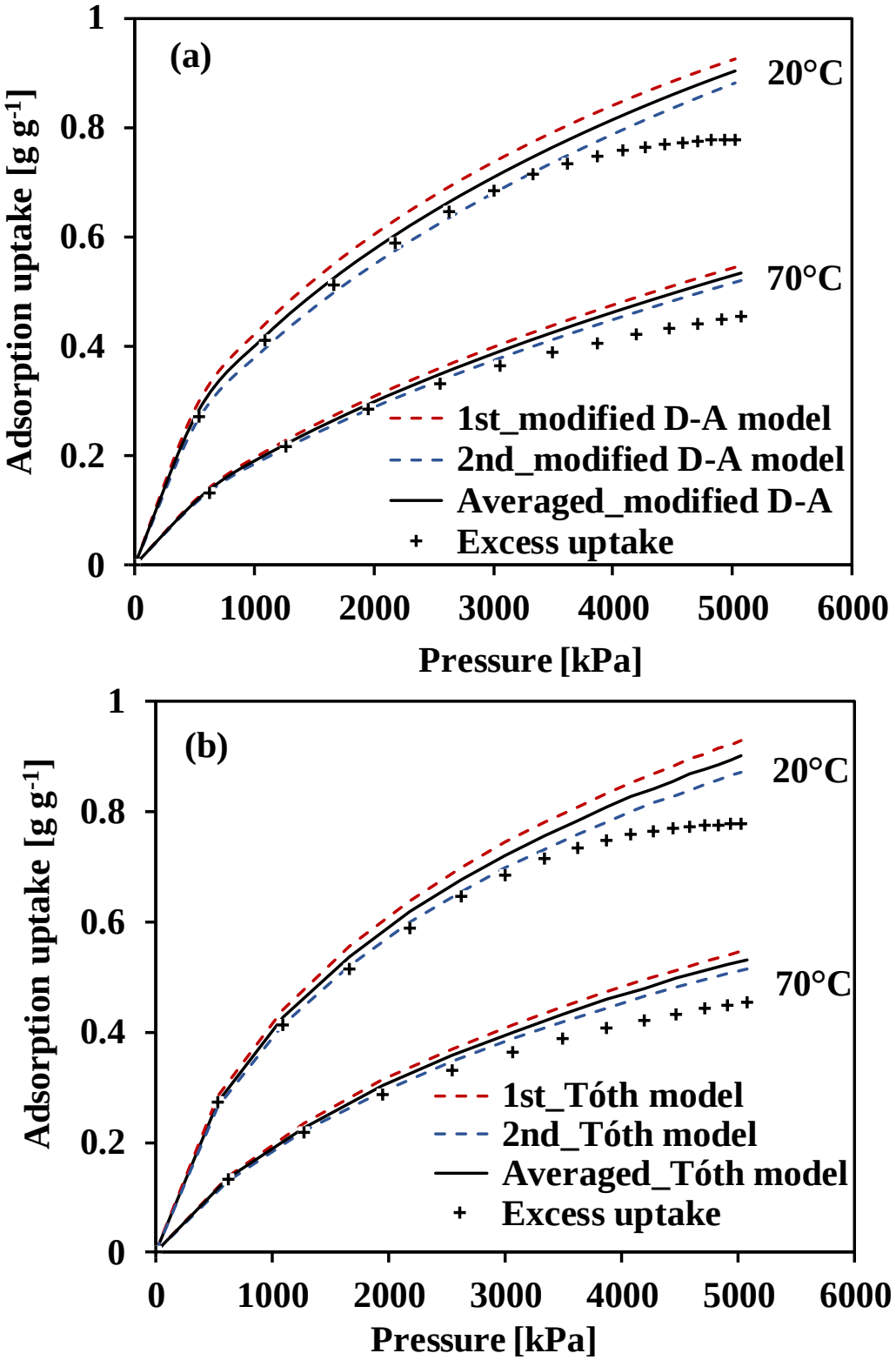

Figure 14 - (a) Modified D-A; (b) Tóth isotherm model and experimental excessive adsorption uptake

5 ISOSTERIC HEAT OF ADSORPTION

Tóth equation includes isosteric heat of adsorption Q as a fitting parameter which is defined during correlation stage. Therefore, the value of Q is constant and doesn't depend on the surface coverage. However, when the isosteric heat of adsorption derived from modified D-A model, it is found as a function of surface coverage, $\theta = C/C_0$. D-A model is one of few models that accounts for adsorbed phase volume changes and uptake dependence of isosteric heat of adsorption variations [69]. Clausius-Clapeyron (C-C) equation, Eq. 21, is used to establish the dependency between the surface coverage θ and isosteric heat of adsorption Q [70].

$$Q = RT^2 \left(\frac{\partial \ln p}{\partial T}\right)_{\text{const}\,\theta} = R\left(\frac{\partial \ln p}{\partial \left(\frac{1}{T}\right)}\right)_{\text{const}\,\theta} \tag{21}$$

The C-C plot is constructed via reverse calculation of pressure for varying temperatures at constant surface coverage θ via Eq. 22.

$$\ln p = \ln\left[\left(\frac{T}{T_c}\right)^k P_c\right] - \frac{E}{RT}\sqrt[m]{\ln\frac{W_0}{CV_t \exp(\alpha(T - T_t))}} \tag{22}$$

Figure 15 shows C-C plot constructed in terms of $\ln p$ versus $1/T$ from generalized D-A model. Tangential of each line corresponding to constant uptake linearly depends on the isosteric heat of adsorption, Eq. 21.

Comparison of isosteric heat of adsorption values estimated from Tóth and modified D-A models are plotted in figure 16. Average value of Q estimated using modified D-A model is 19.742 kJ mol^{-1}, and using Tóth model is 19.023 kJ mol^{-1}. The heat of adsorption value of the synthesized composite/CO_2 pair is having close resemblance with other conventional carbon based adsorbent/CO_2 pairs, which is given in table 7.

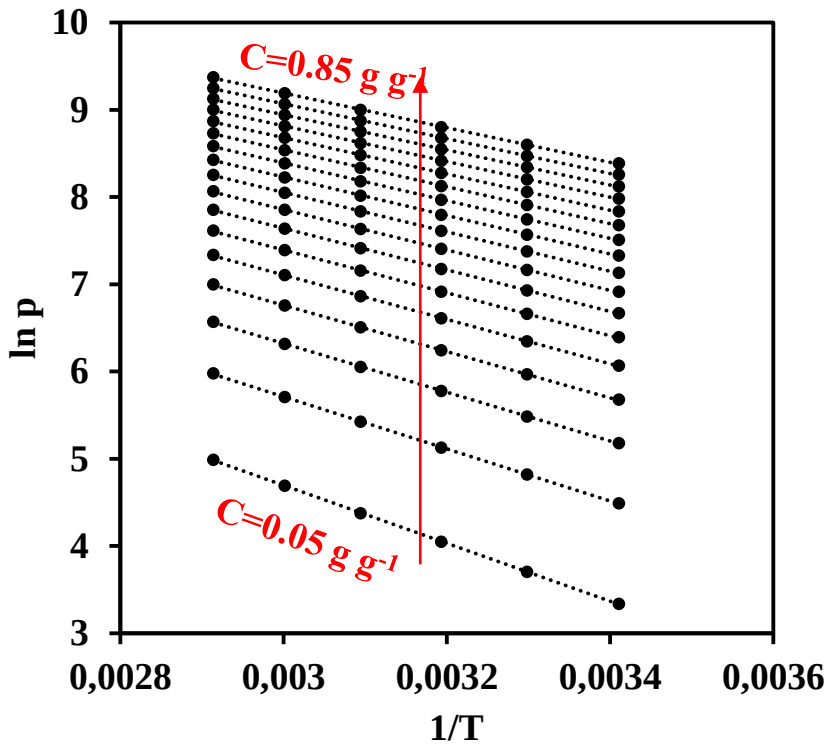

Figure 15 - Clausius-Clapeyron (C-C) plot constructed using modified D-A model

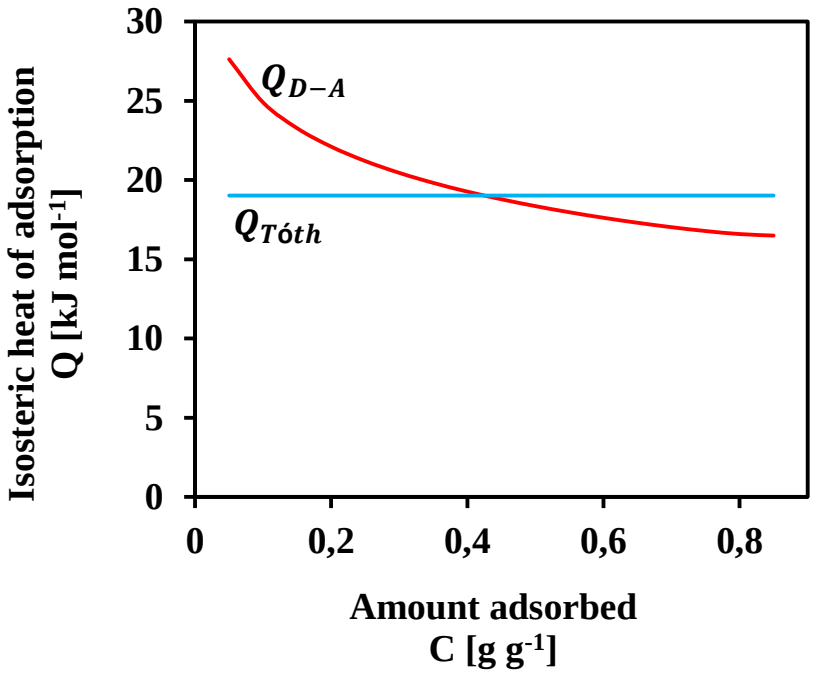

Figure 16 - Isosteric heat of adsorption versus adsorption uptake

However, the perfect gas assumption in estimating the heat of adsorption using Clausius-Clapeyron equation is only valid at low pressures and may result in significant errors for high pressure adsorption applications. Even at partial vacuum

adsorption, Shen et al. [71] observed a discrepancy of around 2kJ mol^{-1} between the calorimetry method predictions by the Clausius-Clapeyron equation. Askalany and Saha [72] presented a theoretical framework for precise determination of the isosteric heat of adsorption for non-ideal gases. Rahman et al. [70, P. 120] proposed Eqs. 23 and 24 to measure Q_{st} at pressures lower and higher than critical pressures respectively. The results are presented in figure 17. It is observed that Q_{st} decreases with increase in uptake and at temperatures higher than T_c, the heat of adsorption value is much higher. A similar trend is also found in literature [73].

$$Q_{st} = h_{fg} + E\left\{(-\ln\theta)^{\frac{1}{n}} + \frac{T\alpha}{n}(-\ln\theta)^{\frac{1}{n}-1}\right\} \tag{23}$$

$$Q_{st} = kRT + E\left\{(-\ln\theta)^{\frac{1}{n}} + \frac{T\alpha}{n}(-\ln\theta)^{\frac{1}{n}-1}\right\} \tag{24}$$

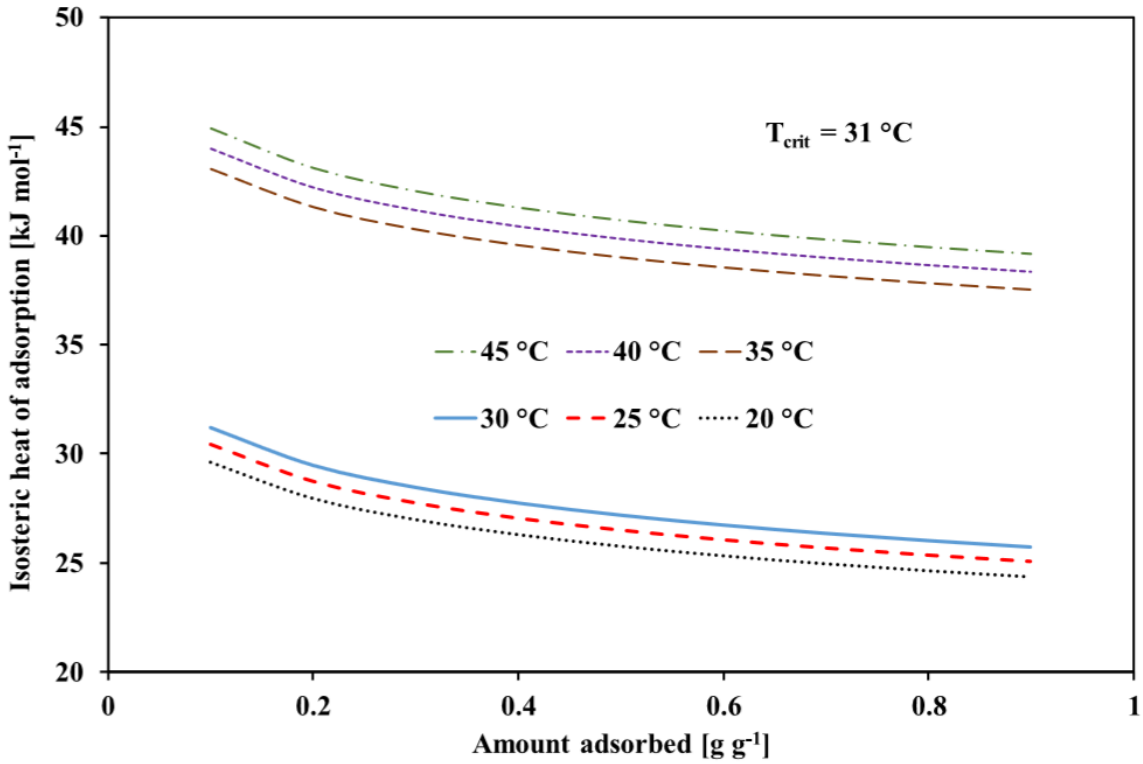

Figure 17 - Isosteric heat of adsorption

Table 7 - Comparison of maximum CO_2 uptake, isosteric heat of adsorption, surface area, pore volume and thermal conductivity of different adsorbents

Adsorbent/CO_2	Maximum uptake (using modified D-A model) [cm^3 g^{-1}]	Isosteric heat of adsorption [kJ mol^{-1}]	Surface area [m^2 g^{-1}]	Pore volume [cm^3 g^{-1}]	Thermal conductivity [W m^{-1} K^{-1}]	Reference
Composite	1.015	19.023	1778	1.014	0.22	Present study
Maxsorb III	1.5408	19.30	3045	1.70	0.066	[39, P. 1944, 42, P. 1219]
A-20 (ACF)	1.03	19.23	2000	1.03	-	[74]
Composite	1.109	22.5	2000	1.094	0.24	[8. P. 310-311]
Norit R1 Extra	0.67	22.0	1450	0.47	-	[75]
BPL	0.51	25.7	1150	0.43	-	[75, P. 369-375]
A10 fiber	0.54	21.6	1200	0.59	-	[75, P. 369-375]
Activated carbon A	0.55	17.8	1207	0.54	-	[75, P. 369-375]
Norit RB3 (AC1)	1.09	15.51	987.04	0.51	-	[76]
Norit Darco (100 mesh size) (AC2)	0.898	16.27	876.45	0.73	-	[76, P. 290-304]
Norit Darco (12 × 20 US mesh size) (AC3)	0.62	16.53	462.67	0.50	-	[76, P. 290-304]
CSAC	0.55	16.44	804.02	0.43	-	[77, 78]

6 ADSORPTION KINETICS

Figure 18 shows the adsorbed mass and pressure changes with time for the experiment on measuring 20 °C isotherm curve. During the experiment new portions of gas entered the sample holding chamber after reaching the complete equilibrium. The constant heat removal allowed measuring the uptake under isothermal conditions. The moments of entering new portions of gas corresponds to the characteristic steps on adsorption mass curve. The experiments continued till reaching 5 MPa in the sample holding chamber. Figure 19 illustrates the instantaneous adsorbed mass versus time for equilibrium pressures from 1-5 MPa with the step of around 1MPa. The curves obtained during the experiment on measuring 20 °C adsorption isotherm.

6.1 Isothermal axial dispersed plug flow model

There are numerous kinetic models to describe gas adsorption: LDF with a single effective mass transfer coefficient [79]; Maxwell-Stefan model with multiple parameters for taking into account the contribution of such mass transfer mechanisms as surface diffusion, viscous flow and Knudsen diffusivity [80]; models with the resistence to mass transport in the macropores. Rashidi et al. [46, P. 440] modeled CO_2 adsorption onto activated carbon using four different models: a pseudo-first order (LDF) and pseudo-second order, Elovich's kinetic model, and an intra-particle diffusion model. Correlation revealed the pseudo-second order model fits well with the kinetic data. Mohammad et al. [81] investigated adsorption kinetics of carbon dioxide but onto activated alumina using additionally to the models mentioned above the Ritchie second order method and the rate controlling kinetic model. The rate controlling model and Elovich's equation show good agreement with experimental data for two sorts of activated alumina respectively. Balsamo et al. [47, P. 214] investigated adsorption kinetics of CO_2 onto synthetic nanoporous activated carbon. In [82] the LDF model showed good prediction for composite/ethanol pair compared to the Fickian diffusion model. As we see there are many different models of varying complexity in the literature, among them the LDF is often used in recent studies because of its simplicity. The LDF model was first proposed by Gluekauf [12, P. 436, 83], Eq. 25. Where, q – instantaneous uptake [$g\ g^{-1}$], t - the time [sec], k - the mass transfer coefficient [sec^{-1}]. In the integrated form, Eq. 26, it allows estimating first approximation for the mass transfer coefficient k by fitting the curve to the experimental data.

$$\frac{dq}{dt} = k\left(q_{eq} - q\right) \tag{25}$$

$$\left| \begin{array}{ll} t = 0 & q(0) = q_{in} \\ t \to \infty & q(\infty) = q_{eq} \end{array} \right.$$

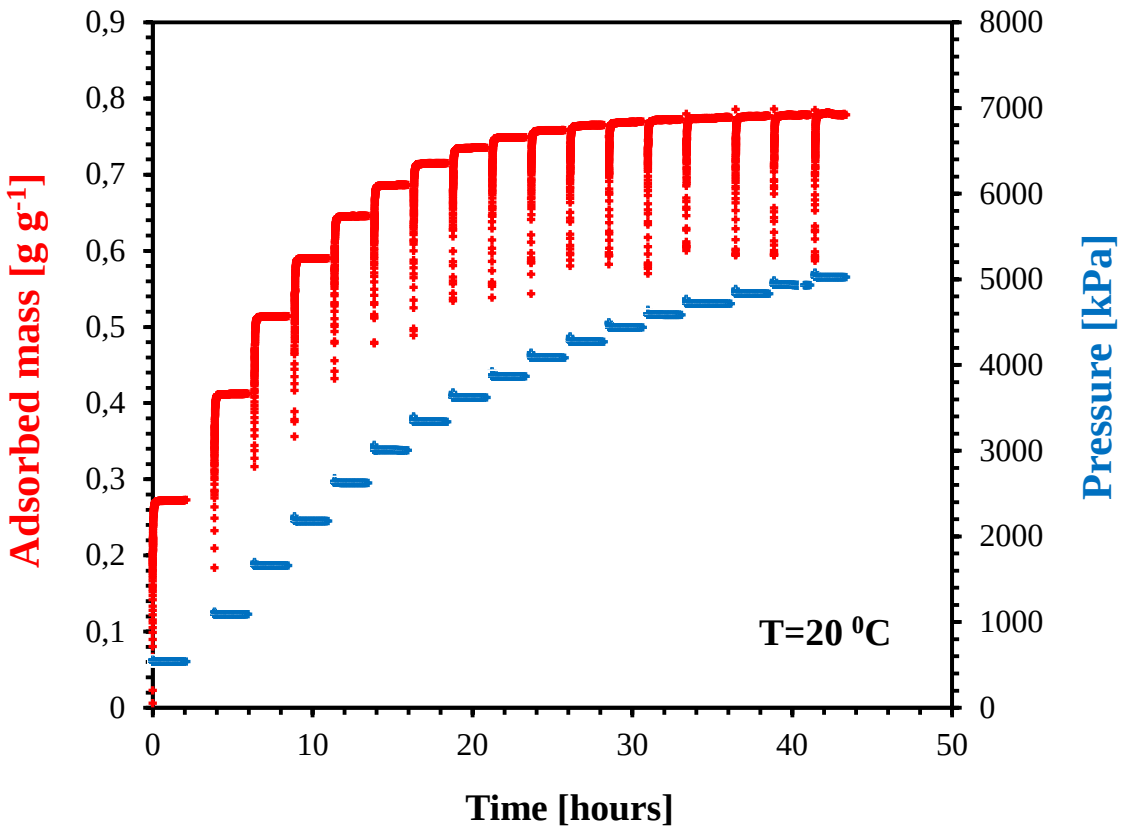

Figure 18 - Adsorbed mass and pressure curves for 20 °C isotherm

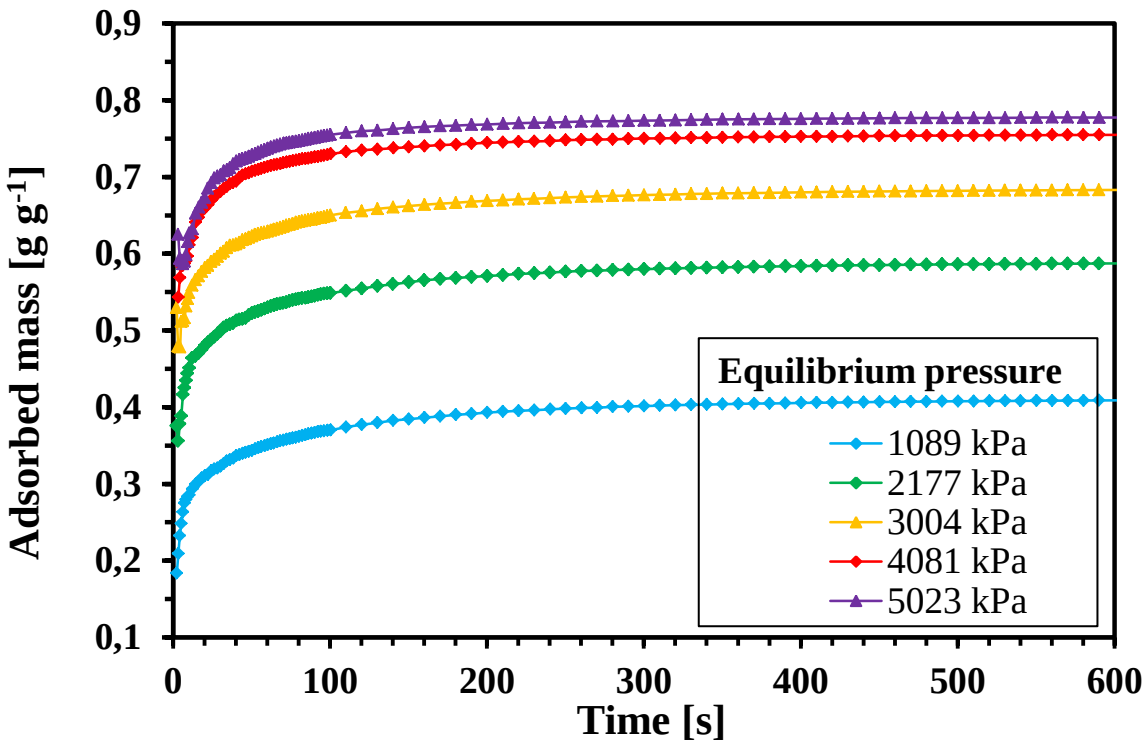

Figure 19 - Experimental instantaneous uptakes for different equilibrium pressures obtained during the experiment for 20 °C isotherm

$$\frac{q - q_{in}}{q_{eq} - q_{in}} = 1 - \exp(-k \cdot t) \tag{26}$$

The classical mass transfer coefficient k is found from surface diffusivity D_s, adsorbent particle radius R_p and a geometric parameter that depends on the adsorbent particle shape F_0, Eq. 27. El-Sharkawy [84] proposed form of the LDF with temperature dependent correction factor in order to improve the accuracy of the classical LDF model, Eq. 28. For simplicity the $\frac{D_s t}{R_p^2}$ is denoted as dimensionless time θ, n is the summation index. The proposed LDF modification tested for the adsorption rate onto the granular adsorbent with spherical particles, and demonstrated good accuracy.

$$k = \frac{F_0 D_s}{R_p^2} \tag{27}$$

$$\frac{q - q_{in}}{q_{eq} - q_{in}} = 1 - \exp\left(-F_0 \left(\frac{T}{T_c}\right)^n \theta^m\right) \tag{28}$$

Buzanowski and Yang [85] proposed extended linear driving-force approximation. Jribi et al. [28] suggested a modified LDF equation with a mass transfer coefficient that is the function of the equilibrium and instantaneous uptakes where the constant k_2 is obtained from experimental data.

$$k_{m.LDF} = f(q_{eq}, q) = k_2^{\frac{q}{q_{eq}}} \tag{29}$$

Some system configurations allow describing the adsorption dynamics using only LDF mass transfer rate model. It works well for granular AC as the adsorption occurs almost uniformly in the pellets thanks to the presence of voids between particles. For the cases of large industrial units the LDF model is solved in pair with the mass balance equation for mobile gas phase [49, P. 2313].

When modeling mass transfer in granular activated carbon, the equation for the transfer of molecules is given in two stages [86]: 1) *transfer in macropores* – transfer of a substance between the granules of the adsorbent, the pellet diameter usually varies between 500-1000 μm, Eq. 30; 2) *transfer in micropores* – transfer of the substance inside the pellet of the adsorbent, Eq. 31.

$$\varepsilon_b \frac{\partial c_A}{\partial t} = \varepsilon_b D_L \frac{\partial^2 c_A}{\partial z^2} - \varepsilon_b u_g \frac{\partial c_A}{\partial z} + (1 - \varepsilon_b) k_f \frac{3}{r_p}(c_A - c_p) \tag{30}$$

$$\varepsilon_p \frac{\partial c_p}{\partial t} = D_m \left(\frac{1}{r^2}\frac{\partial}{\partial r}\left(r^2 \frac{\partial c_p}{\partial r}\right)\right) - (1 - \varepsilon_p)\rho_{sk} \frac{\partial q}{\partial t} \tag{31}$$

$$\frac{\partial q}{\partial t} = k\left(q_{eq} - q\right) \tag{32}$$

$$q_{eq} = \frac{q_{max} bP}{1 + bP} \tag{33}$$

In case of consolidated activated carbon, the gas phase transfer is given in one stage; therefore we have the following system of PDEs, Eqs. 34-37.

$$\varepsilon_p \frac{\partial C}{\partial t} = \frac{\partial J_K}{\partial z} - \left(1 - \varepsilon_p\right)\rho_{sk} \frac{\partial q}{\partial t} \tag{34}$$

$$\text{or} \quad \varepsilon_p \frac{\partial C}{\partial t} = D_m \frac{\partial^2 C}{\partial z^2} - \left(1 - \varepsilon_p\right)\rho_{sk} \frac{\partial q}{\partial t} \tag{35}$$

$$\frac{\partial q}{\partial t} = k\left(q_{eq} - q\right) \tag{36}$$

$$q_{eq} = \frac{q_{max} b_0 e^{\frac{E}{RT}} P}{1 + b_0 e^{\frac{E}{RT}} P} \tag{37}$$

The mathematical model was solved for 1D axial dispersed plug flow case. The length of the plug is $z = 2\ cm$. The calculation domain schematically illustrated in figure 20. Adsorption breakthrough curves and gas diffusion/penetration dynamics illustrated there below. The system of PEDs discretized using explicit difference scheme. Langmuir constants were taken from [68, P. 239]: the maximum absorption $q_{max} = 1.13016\ g\ g^{-1}$, the equilibrium constant $b_0 = 1.238 \cdot 10^{-7}\ kPa^{-1}$, the heat of adsorption $E = 20751\ J\ mol^{-1}$. The Dirichlet boundary condition applied for the gas concentration at the left boundary and set to be equal to the equilibrium concentration $C(z = 0, t) = C_{eq},\ C_{eq} = 0.00968\ g/cm^3$. The amount of adsorbed substance per unit volume of adsorbent according to the initial condition $q(z, t = 0) = 0$ at the initial time is zero, and rises over time as shown in figure 20. The gas diffuses into the adsorbent according to the graph of gas phase concentration curves over time. Molecules migrate into a porous medium due to Knudsen diffusion. The initial condition for the mobile/gas phase concentration was also set equal to zero $\mathrm{C}(z, t = 0) = 0$, which corresponds to a complete vacuum. The results obtained reasonable and correspond to the expected behavior at diffusion transfer. Although results illustrated for the first 10 seconds only, the equilibrium in the system equilibrium in the system is established at about 10 minutes. This is indicated as an instant when adsorption uptake reaches the plateau, $q_{eq} = 0.12815\ g/cm^3$. Axial dispersed plug flow model also discussed in [87].

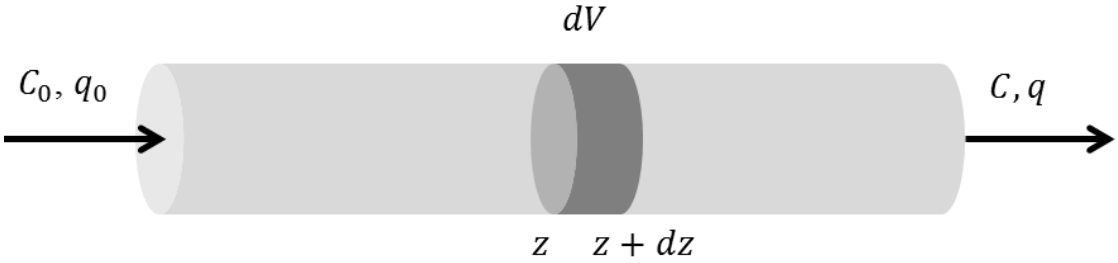

(a)

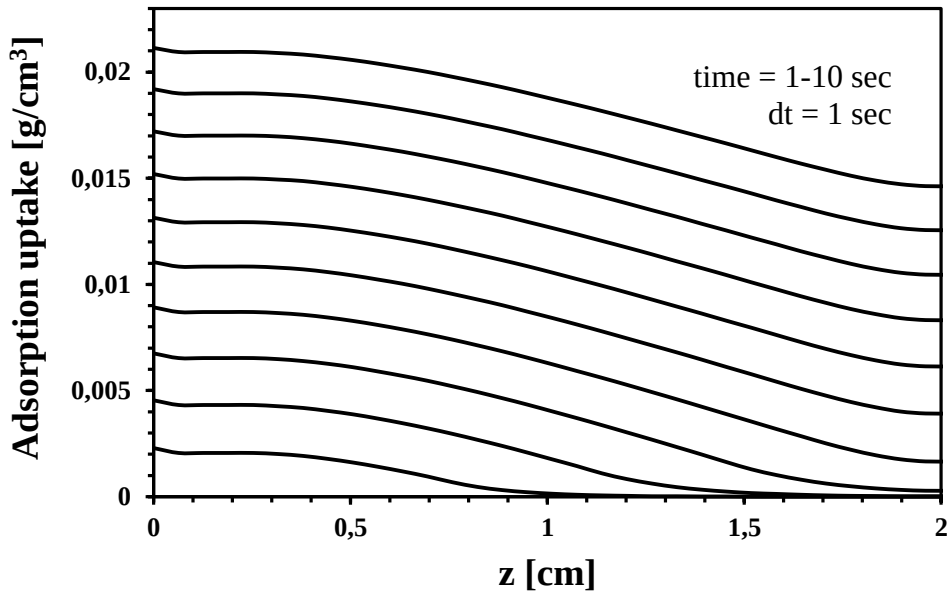

(b)

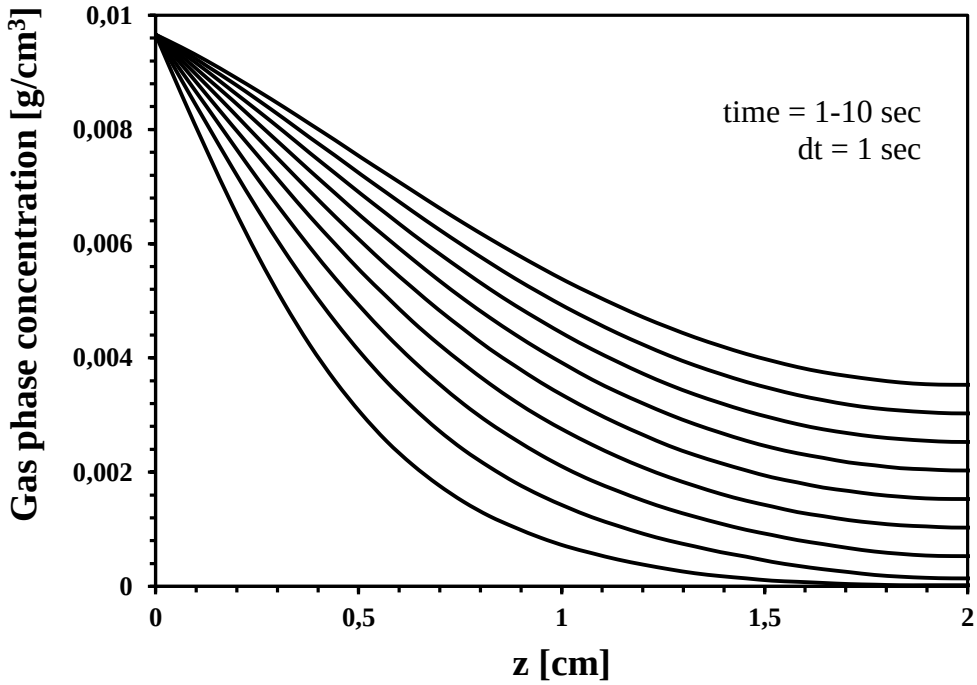

(c)

Figure 20 - (a) Schematic illustration of the calculation domain. (b) The mass of the absorbed substance per unit volume of adsorbent. (c) Gas diffusion/penetration dynamics into the sorbent. The mass of the CO_2 in the gas phase per unit volume of adsorbent

6.2 Effective Knudsen diffusivity

According to the figure 4 the main part of the voids occupied with the pores of diameter up to 30 Å. In such system the Knudsen diffusion takes place, which differs from continuum diffusion in that the collision of gas molecules with the walls of the porous medium is dominant than the collision of gas molecules with each other. The adsorbate molecules diffuse into the porous media because of the concentration gradient, and the parameter characterizing this transfer is called the Knudsen diffusion coefficient. The Knudsen flux depends on the pore size distribution $f(r)$ and the molecular weight of the adsorbate, M, since the molecules with lower weight move faster than molecules with higher weight under the same concentration gradient. Effective Knudsen diffusion coefficient for porous media given in Eqs. 38-40 [88-89]. Eq. 40 is for Knudsen diffusivity in capillary tube of certain radius; it depends on the radius of the tube, the molecular weight and temperature of the diffusing gas molecule. By representing the porous media as a bunch of capillary tubes of known pore size distribution (figure 21) the effective Knudsen coefficient is estimated by Eq. 39.

$$J_K = -D_{K\_eff}\frac{dC}{dz} \tag{38}$$

$$D_{K\_eff} = \frac{\varepsilon}{\tau^2}\left[\int_0^\infty D_K(r)\cdot f(r)dr\right] \tag{39}$$

$$D_K = \frac{2r}{3}\sqrt{\frac{8R_gT}{\pi M}} \tag{40}$$

The tortuosity of porous media depends on the porosity, shape and connectivity of pores [90]. In the present research the equation that works well to find tortuosity of the porous media $\tau = \varepsilon^{-0.5}$ was applied. Calculated effective Knudsen diffusivity coefficient for the working pair at the temperature 293.15 K is $D_{K\_eff} = 2.644\cdot 10^{-3}\ cm^2\ s^{-1}$. For comparison in [91] the Knudsen diffusion coefficient for nanoporous media and shale gas system is found to vary from $7.0\cdot 10^{-2}$ to $10.0\cdot 10^{-2} cm^2\ s^{-1}$. In [92] the effective Knudsen diffusivity is found ranging between $10^{-2} - 10^{-3}\ cm^2\ s^{-1}$ for ethane and propane molecules in the activated carbon. Hu and Liu [93] observed the diffusivity of CO_2 on MFI zeolite decreases with the increase of amount of adsorption. The diffusivity coefficient almost linearly decreased from $0.7\cdot 10^{-4}$ to $0.2\cdot 10^{-4}\ cm^2\ s^{-1}$ for uptakes varying between 0.5 – $3.0 mmol\ g^{-1}$. Ribeiro et al. [49, P. 2315] obtained diffusion coefficient of CO_2 in an activated carbon honeycomb monolith to be $2.28\cdot 10^{-3}\ cm^2\ s^{-1}$.

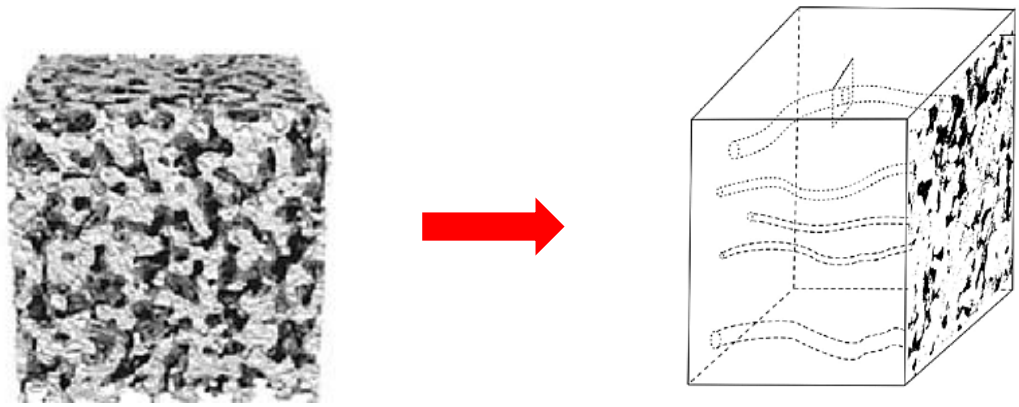

Figure 21 - Porous media representation as a bunch of capillary tubes

6.3 TGA experiment simulation using isotermal model

Knudsen coefficient decreases with uptake, as less space becomes available for bulk gas molecules, and molecular diffusion into the sample becomes more difficult. But the assumption $D_{eff} = const$ is acceptable for the cases when the equilibrium occurs at low adsorption coverage θ. Also the void fraction ε is taken as constant in most research works. The model was compiled using the following assumptions: a) the process is isothermal, b) adsorption of pure CO_2 considered, c) the gas and adsorbed phase are in the thermal equilibrium, d) the porosity stays constant with adsorption. Material balance equation, Eq. 41 or 42, discretized using the explicit finite difference scheme and complied with, $Currant < 1$ stability condition, Eq. 43.

$$\varepsilon \frac{\partial C}{\partial t} = D_{Kn} \nabla^2 C - (1-\varepsilon)\rho_{sk} \frac{\partial q}{\partial t} \tag{41}$$

or

$$\frac{\partial C}{\partial t} = \frac{D_{Kn}}{\varepsilon}\left(\frac{\partial^2 C}{\partial x^2} + \frac{\partial^2 C}{\partial y^2} + \frac{\partial^2 C}{\partial z^2}\right) - \frac{(1-\varepsilon)\rho_{sk}}{\varepsilon}\frac{\partial q}{\partial t} \tag{42}$$

$$\frac{D_{Kn} \cdot \Delta t}{\Delta z^2} \leq \frac{Currant}{6} \tag{43}$$

The cylinder shaped tablet for the sake of simplicity was modeled as a cube with sides $a = 0.742\ cm$ (figure 22). Porous materials have two densities, apparent (or packing density) and true (or skeletal density). The skeletal density is experimentally measured by gas pycnometer, discussed in [94]. The skeletal density for the given composite is $\rho_{sk} = 0.917\ g\ cm^{-3}$. Packing density is the ratio of mass to the sample's volume, for the current composite is $\rho_{pack} = 0.475\ g\ cm^{-3}$. The sample's porosity $\varepsilon = 0.482$.

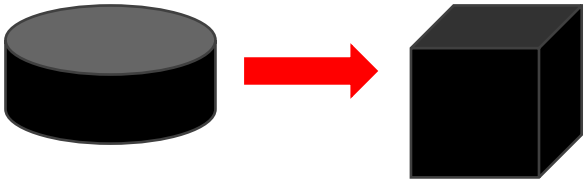

Figure 22 - Schematic illustration of the calculation domain

The first step in the adsorbed mass curve for 20°C isotherm corresponding to the equilibrium/saturation pressure 535 kPa was considered for simulation. Dashed line in figure 25 is the instantaneous adsorption uptake obtained experimentally. Figure 23 (left column) illustrates the distribution of adsorbed phase concentration over the sample volume at time instants 1.035sec, 3.105 sec and 5.175 sec. The finite elements at the borders of the sample are more saturated than elements in the center. Figure 23 (right column) illustrates the gas phase concentration distribution throughout the sample's volume.

When comparing numerical data with experimental the average is more informative. By integrating instantaneous numerical absolute uptake throughout the body and dividing by its volume *the numerical specific absolute uptake* is calculated, Eq. 44. Mass transfer coefficient is correlated by fitting the numerical and experimental specific uptakes, and the best fit corresponds to $k = 0.013\ sec^{-1}$.

$$\bar{q} = \frac{\int q\ dV}{V} \tag{44}$$

Figure 25 shows the numerically obtained average adsorption uptake $\bar{q}$ over time till saturation moment using non-reactive isothermal model. The discrepancy of the experimental and numerical adsorption uptake is due to the model assumptions. (i) The void fraction available for the gas phase ε is constant, i.e. with gas absorption the porosity of the sample remains the same. (ii) The Knudsen diffusivity coefficient stays constant with adsorption. Since the saturation volume of adsorbed phase is less than 15% of pore volume of the sample, neglecting these effects assumed not to affect much on the result. But for higher pressures when the saturation adsorption tends to the maximum uptake those effects should be taken into account. (iii) As explained in [27, P. 67] the sharp increase of adsorption uptake at adsorption starting causing adsorbent temperature increase due to released heat of adsorption. The isothermal model doesn't consider temperature changes due to the adsorption, as higher the temperature lower the adsorption potential. Therefore the discrepancy also caused by the use of isothermal model. (iv) During the experiment, after injecting another portion of gas the pressure at the sample holding chamber increases sharply and gradually tends to plato with gas adsorption, whereas in the model the pressure in the boundary sides set to be constant. This explains sharp increase of adsorption uptake at adsorption starting.

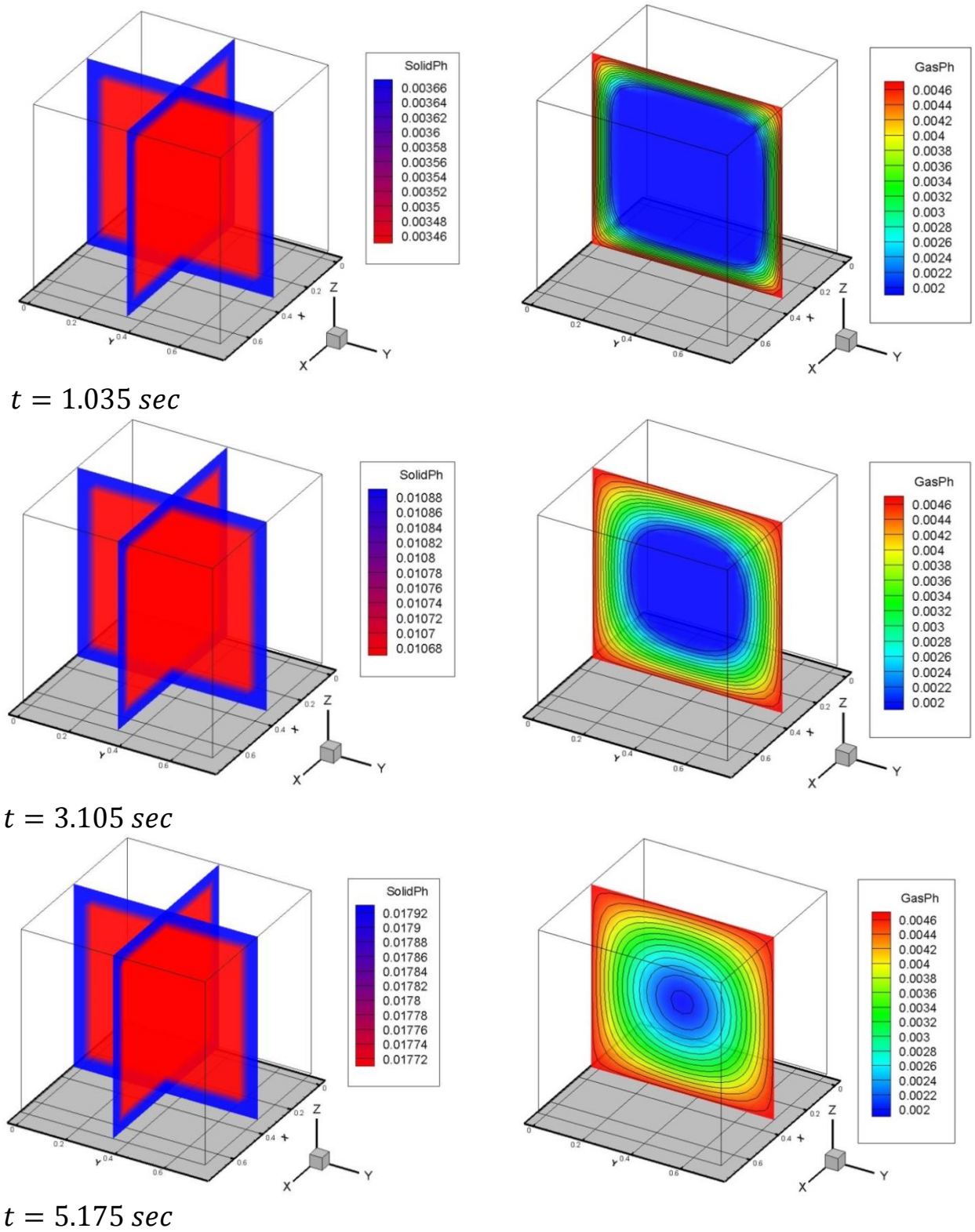

Figure 23 - Left column: Mass of adsorbed substance per unit mass of sorbent. Right column: Mobile/gas phase concentration dynamics. Amount of moles of the substance per unit volume of the sorbent

The values of mass transfer coefficient from literature for similar systems for comparison are furnished below. Jribi et al. [27, P. 64] fitted the TGA experimental data to isothermal LDF model and found optimum mass transfer coefficient (in the paper referred as the diffusion time constant) as 0.0043 sec^{-1} for ethanol adsorption onto AC powder of type Maxsorb III for adsorption temperature 30^0C, at initial pressure of 1.71 kPa and charging pressure of 2.25 kPa. They mentioned that isothermal adsorption simulation under-estimates the mass adsorbed compared to experimental data, the divergence is due to the sharp increase of adsorption uptake at adsorption starting causing adsorbent temperature increase due to released heat of adsorption. Unfortunately, experimentally temperature variation of the adsorbent is not known. Authors presented the non-isothermal kinetics equation: the mass transfer coefficient set via temperature dependent Arrhenius equation, the temperature variation implemented using energy balance equation with the use of isosteric heat of adsorption.

Dantas et al. [79, P. 80] studied the adsorption of diluted CO_2 in helium onto commercial granular AC. Two different molar fractions 0.1 and 0.2 were used in the experiment. The numerical simulation reproduced the experimental curves well at mass transfer coefficients of 0.0027 sec^{-1}, 0.0043 sec^{-1}, 0.0125 sec^{-1}, 0.0259 sec^{-1} at four different temperatures 301 K, 323 K, 373 K, and 423 K respectively.

6.4 Non-isothermal reactive axial dispersed plug flow model

Chadam et al. [95] demonstrated mathematical model for the reactive flow in porous media. The developed mathematical model considers the reaction caused porosity/permeability changes in the porous media and viscosity changes in the fluid. In the present research the abovementioned mathematical model was modified and adjusted to the case of adsorptive flow of gas through nanoporous media Eqs. 53-56. Developed model considers the adsorption caused porosity and Knudsen diffusivity changes to apply for the cases when the volume of the adsorbed phase becomes comparable with the pore volume available. And the mass transfer coefficient $k(T)$ is the temperature dependent function. Derivation of mass balance equation for mobile gas is following. Eq. 46 describes the flux caused by concentration gradient during the Knudsen regime for multidimensional case. The amount of gas which is adsorbed and transferred to the solid phase balance is expressed as Eq. 47, and corresponds to the sink term in the mass conservation equation Eq. 48.

$$m = \int_V \varepsilon_p \cdot C \cdot dV \tag{45}$$

$$\bar{J} = -D_{Kn}(\varepsilon_p) \cdot \nabla C = -D_{Kn}(\varepsilon_p) \cdot \nabla C \cdot \bar{n} \tag{46}$$

$$\dot{f} = -(1 - \varepsilon_{p,0})\rho_{sk} \frac{\partial q}{\partial t} \tag{47}$$

$$\frac{d}{dt}\int_V \varepsilon_p \cdot C \cdot dV = \int_S \bar{J}\, dS - \int_V \dot{f}\, dV \tag{48}$$

Therefore

$$\frac{d}{dt}\int_V \varepsilon_p \cdot C \cdot dV = \int_S -D_{Kn}(\varepsilon_p) \cdot \nabla C \cdot \bar{n}\ dS - \int_V \dot{f}\, dV \tag{49}$$

$$\int_V \frac{\partial(\varepsilon_p \cdot C)}{\partial t} dV = \int_V \nabla \cdot (-D_{Kn}(\varepsilon_p) \cdot \nabla C)\, dV - \int_V \dot{f}\, dV \tag{50}$$

$$\int_V \frac{\partial(\varepsilon_p \cdot C)}{\partial t} dV = \int_V \nabla \cdot (-D_{Kn}(\varepsilon_p) \cdot \nabla C)\, dV - \int_V \dot{f}\, dV \tag{51}$$

$$\int_V \left(\frac{\partial(\varepsilon_p \cdot C)}{\partial t} - \nabla \cdot \left(-D_{Kn}(\varepsilon_p) \cdot \nabla C\right) + \dot{f}\right) dV = 0 \tag{52}$$

As a result material balance equations are described as:

$$\frac{\partial(\varepsilon_p \cdot C)}{\partial t} = \nabla \cdot \left(-D_{Kn}(\varepsilon_p) \cdot \nabla C\right) - \left(1 - \varepsilon_{p,0}\right)\rho_{sk}\frac{\partial q}{\partial t} \tag{53}$$

$$\frac{\partial q}{\partial t} = k(T)\left(q_{eq} - q\right) \tag{54}$$

For the concentration of the mobile phase at the upper boundary of the tablet, the Dirichlet condition is set, as the gas concentration at the boundary is maintained constant and equal to the equilibrium concentration. At the lower boundary of the sample the condition of impenetrability is set. Therefore the boundary and initial conditions for mass balance equations are, Eq. 55-58:

$$C|_{t=0} = 0 \tag{55}$$

$$C|_{z=0} = C_{eq} \tag{56}$$

$$\left.\frac{\partial C}{\partial z}\right|_{z=L} = 0 \tag{57}$$

$$q|_{t=0} = 0 \tag{58}$$

During the process of adsorption D_{K_eff} should decrease with uptake, as less space becomes available for mobile gas molecules, and molecular diffusion into the sample becomes more difficult because the shell of the sample saturates first and gets less permeable. Therefore the porosity is the function of uptake $\varepsilon = \varepsilon(q)$, whereas Knudsen coefficient is the function of porosity $Kn = Kn(\varepsilon)$.

$$\frac{\partial \varepsilon_p}{\partial t} = -\frac{1}{\rho_{ads\ phase}} \frac{\partial q}{\partial t} \tag{59}$$

$$D_{Kn}(\varepsilon_p) = \frac{D_{Kn,0}}{\varepsilon_{p,0}} \cdot \varepsilon_p \tag{60}$$

Total energy and the specific energy concluded in the adsorbent sample are given as Eq. 61 and Eq.62 respectively.

$$H = mc_pT \tag{61}$$

$$\rho_{th} = \rho c_pT \tag{62}$$

With the analogy of the mass balance equation the energy balance equation derived by integrating the heat transfer mechanisms occurring in the system over the volume. The amount of heat released with gas adsorption $\dot{f_{th}}$ is given as a source term in the energy conservation equation, Eq. 65.

$$\overline{J_{th}} = -k_{th}(q) \cdot \nabla T = -k_{th}(q) \cdot \nabla T \cdot \bar{n} \tag{63}$$

$$\dot{f_{th}} = \dot{m} \cdot Q_{st} \tag{64}$$

$$\frac{d}{dt} \int_V \rho_{th}\, dV = \int_S \overline{J_{th}}\, dS + \int_V \dot{f_{th}} dV \tag{65}$$

Therefore

$$\frac{d}{dt} \int_V \rho c_pT\, dV = \int_S -k_{th}(q) \cdot \nabla T \cdot \bar{n}\, dS + \int_V \dot{f_{th}} dV \tag{66}$$

$$\int_V \rho c_p \frac{\partial T}{\partial t} dV = \int_V \nabla \cdot (-k_{th}(q) \cdot \nabla T)\, dV + \int_V \dot{f_{th}} dV \tag{67}$$

$$\int_V \left(\rho c_p \frac{\partial T}{\partial t} - \nabla \cdot (-k_{th}(q) \cdot \nabla T) + \dot{f_{th}}\right) dV = 0 \tag{68}$$

$$\rho c_p \frac{\partial T}{\partial t} = \nabla \cdot (-k_{th}(q) \cdot \nabla T) + \dot{f_{th}} \tag{69}$$

With adsorption uptake the specific heat capacity of the material changes. As mentioned in [96-97] the specific heat capacity at various adsorption uptakes $c_p(q)$ is calculated as the sum of the specific heat of dry adsorbent and specific heat of the gas at adsorbed state with appropriate weight fractions. But for non-isothermal process it also depends on temperature and the general expression for the adsorbate-adsorbent pair at various uptakes and temperatures is (Eq. 70):

$$c_p(q,T) = (a_0 + a_1 q + a_2 q^2) + (b_0 + b_1 q + b_2 q^2)T \tag{70}$$

In the given study the thermal conductivity of the material at different uptakes and temperatures was not measured experimentally and not available, therefore in the simulation it is assumed to be constant,

$$\frac{\partial T}{\partial t} = \alpha_{th} \cdot \nabla^2 T + \frac{\dot{f_{th}}}{\rho c_p} \tag{71}$$

The shell of the composite sample exchange heat by convection with the surrounding gas during the adsorption process. The surrounding temperature considered at constant temperature, T_∞. In fact, the chamber temperature is maintained constant by an oil circulator. The free convection heat transfer coefficient of carbon dioxide at different temperatures and pressures is taken as 18 W m^{-2} K^{-1}. Convective heat transfer BC (Eq. 72) is set to the both edges of the given configuration, where, $\theta = T - T_\infty$.

$$h\theta(L) = -k\left(\frac{\partial \theta}{\partial x}\right)_{x=L} \tag{72}$$

The calculation domain simplified to 1D case illustrated in figure 24. The case excludes the gas penetration from the sides of the tablet, as the model is one dimensional and corresponding to the case of tablet with insulated sides.

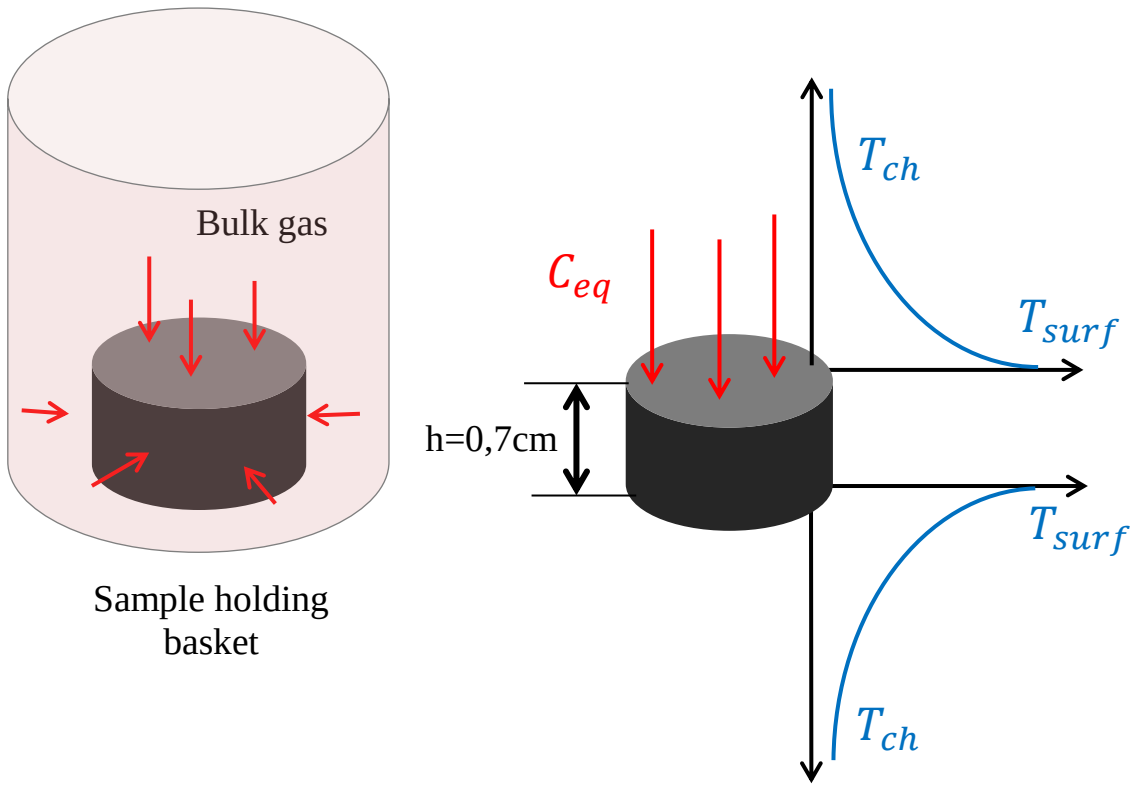

Figure 24 - Calculation domain

The system of equations (table 9) includes two second-order equations, they are the energy balance equation and the mass balance equation for the mobile phase. The remaining equations are of the first order or functions of other variables. For each second-order equation in the mathematical model a time step was determined that satisfies the stability condition, and the smallest was taken in the calculation. In given case, it is 0.025 seconds.

Figure 25 (red line) shows average adsorption uptake $\bar{q}$ over time till saturation calculated using non-isothermal reactive model for axial dispersed plug geometry. Compared to the curve obtained using isothermal model the model illustrates sharp increase at the adsorption starting. The adsorption causes local temperature increase due to released heat of adsorption, as it mentioned before as the process of adsorption is exothermic. The absolute error between experimental data and calculated value is given in figure 26: where blue line is the absolute error for the isothermal model and red line for the non-isothermal reactive model.

The volume averaged temperature change $\bar{T}$ over time (figure 27) shows fast increase in temperature after adsorption begins, with the maximum of 335K at 57 seconds. As higher the temperature as lower the adsorption potential. Therefore till 400 seconds lower rate of mass uptake is observed compared to the isothermal model prediction. Due to the energy dissipation to the surrounding, to the sample holding channel by free convection the mean temperature slowly decreases and equilibrates at 293K.

Figure 28 shows volume averaged porosity change over time. Initially for regenerated sample the porosity is $\varepsilon_0 = 0.482$, after saturation at given pressure and

temperature conditions ($p_{eq} = 535\ kPa, T = 293K$) the final porosity is set at 0.376. The change in mean gas phase concentration over time illustrated in figure 29. Initially the gas concentration is zero within the sample's body, and increase as molecules defund into pores by Knudsen flux. A the very beginning almost all the molecules defunded gets adsorbed by the sample and the front of the gas concentration reaches the second end of the plug (the first breakthrough) in 10 seconds.

Figure 30 - 33 shows dynamics of the instantaneous uptake, the temperature distribution, porosity change and mobile gas concentration along the plug axis. The time step is 9.5 seconds. The calculation performed for the time laps of 900 seconds. In figure 31 the curves corresponding to the moments until the volume averaged temperature reaches its maximum colored black, after the temperature gradually decreases because of energy dissipation to the surrounding.

Table 8 – Assumptions summary

	Isothermal model	Non-isothermal reactive flow model
Assumptions	1. Isothermal system; 2. Porosity is constant; 3. Knudsen diffusivity is constant.	1. Knudsen coefficient linearly depends on adsorption uptake; 2. Thermal conductivity is independent from adsorption uptake.

Table 9 - Mathematical models summary

	Isothermal model	Non-isothermal reactive flow model
System of equations	$$\varepsilon \frac{\partial C}{\partial t} = D_{Kn} \nabla^2 C - (1-\varepsilon)\rho_{sk} \frac{\partial q}{\partial t}$$ $$\frac{dq}{dt} = k\left(q_{eq} - q\right)$$	$$\frac{\partial(\varepsilon_p \cdot C)}{\partial t} = \nabla \cdot \left(-D_{Kn}\left(\varepsilon_p\right) \cdot \nabla C\right) - \left(1 - \varepsilon_{p,0}\right)\rho_{sk} \frac{\partial q}{\partial t}$$ $$\frac{\partial T}{\partial t} = \alpha_{th} \cdot \nabla^2 T + \frac{\dot{f_{th}}}{\rho c_p}$$ $$\frac{\partial q}{\partial t} = k(T)\left(q_{eq} - q\right)$$ $$\frac{\partial \varepsilon_p}{\partial t} = -\frac{1}{\rho_{ads\,phase}} \frac{\partial q}{\partial t}$$ $$D_{Kn}\left(\varepsilon_p\right) = \frac{D_{Kn,0}}{\varepsilon_{p,0}} \cdot \varepsilon_p$$ $$\frac{q_{eq}}{q_0} = \frac{b_0 e^{\frac{Q}{RT}} P}{\left(1 + \left(b_0 e^{\frac{Q}{RT}} P\right)^t\right)^{1/t}}$$

Table 10 - Problem parameters

Parameters	Unit	Value
Knudsen diffusivity coefficient	$cm^2\ sec^{-1}$	0.002644
Surface area	$m^2\ g^{-1}$	1778
Thermal conductivity	$W\ m^{-1}\ K^{-1}$	0.22
Thermal capacity	$J\ g^{-1}\ K^{-1}$	0.8212
Isosteric heat of adsorption	$kJ\ mol^{-1}$	19.023
Porosity	-	0.482
Skeletal density	$g\ cm^{-3}$	0.917
Packing density	$g\ cm^{-3}$	0.475
Temperature	K	293.15
Equilibrium pressure	kPa	535
Equilibrium gas concentration	$g\ cm^{-3}$	0.009656
Equilibrium uptake	$g\ g^{-1}$	0.274

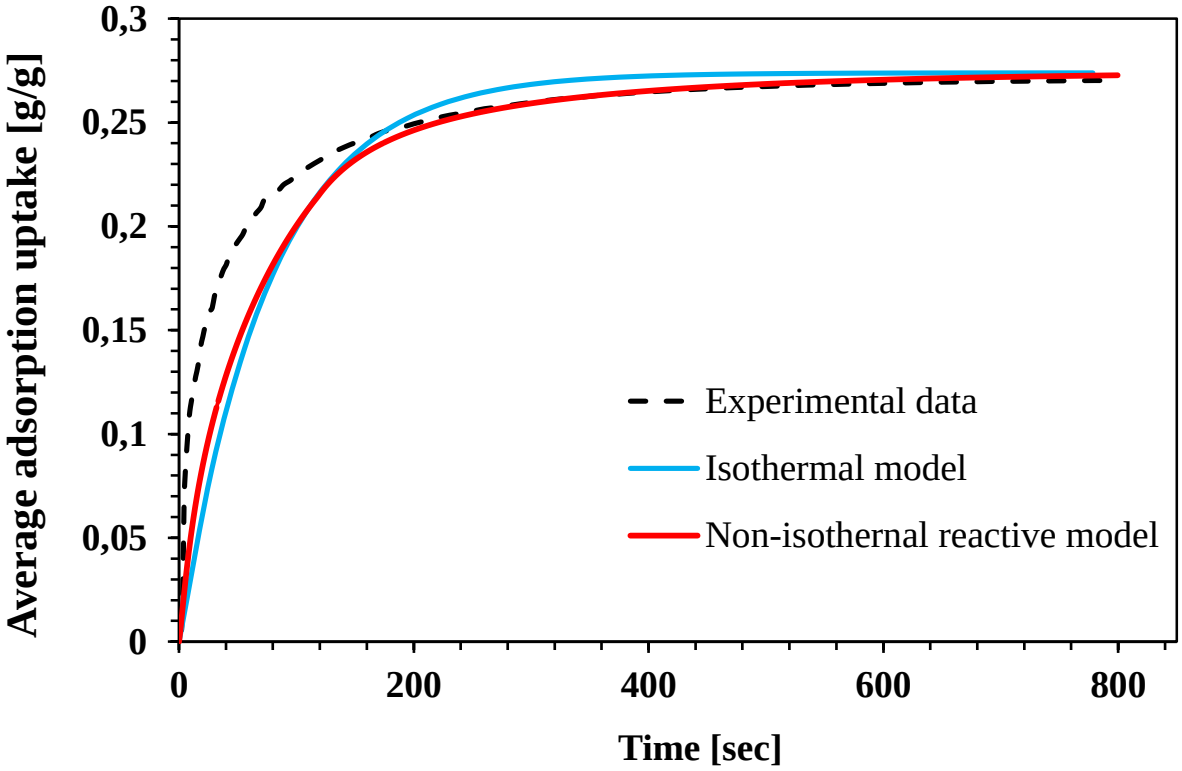

Figure 25 - Volume averaged adsorption uptake. Blue line – uptake calculated using isothermal model, red line – uptake calculated using non-isothermal reactive model

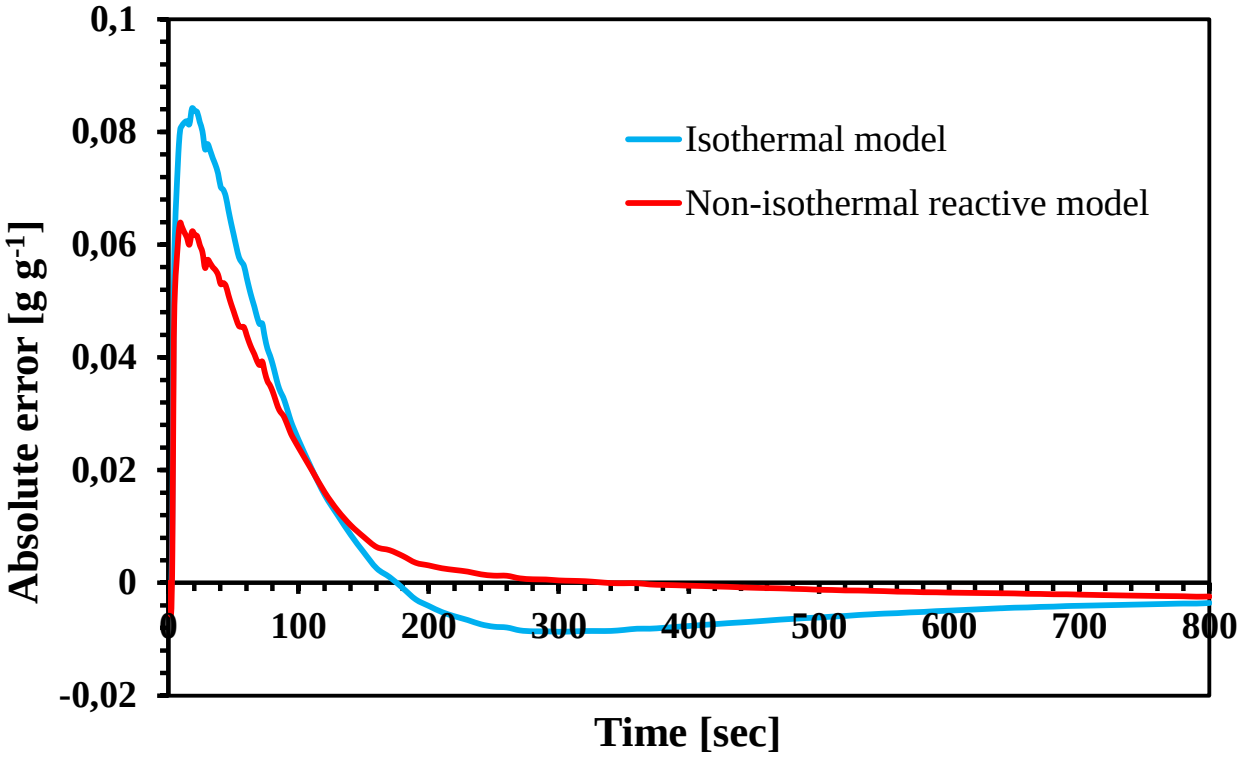

Figure 26 - The difference between the calculated and experimental value. Blue line – absolute error of the isothermal model, red line – absolute error of the non-isothermal reactive model

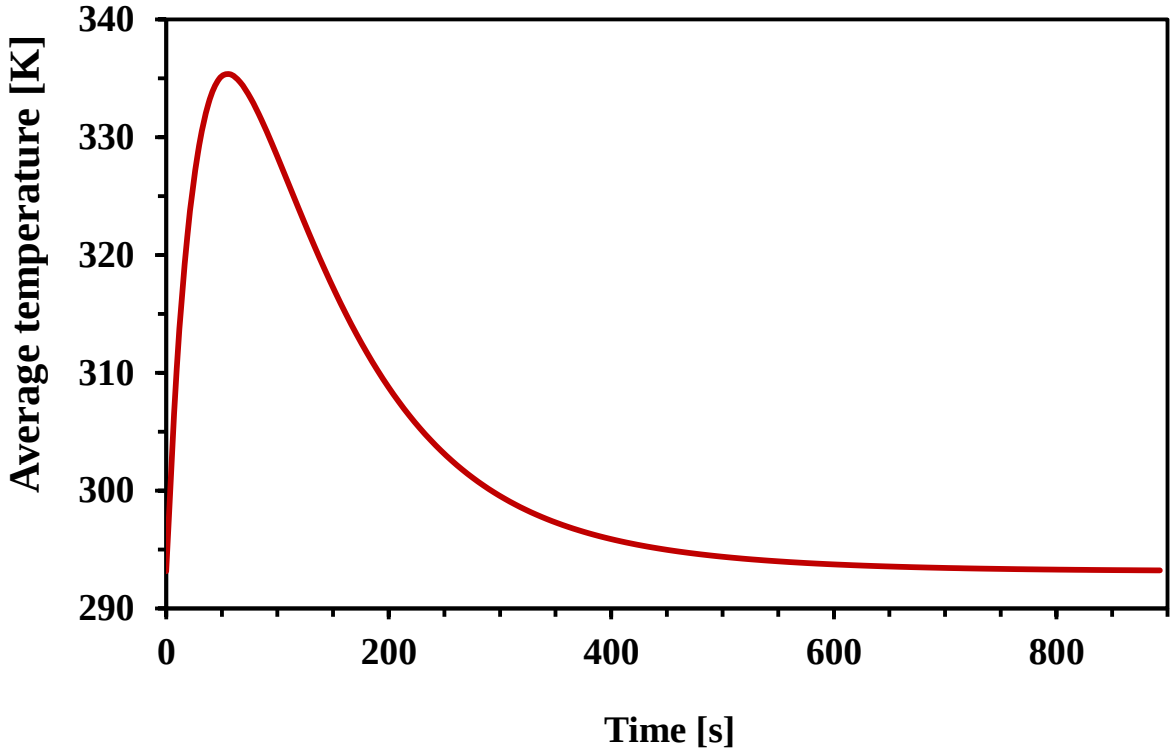

Figure 27 - Volume averaged temperature profile

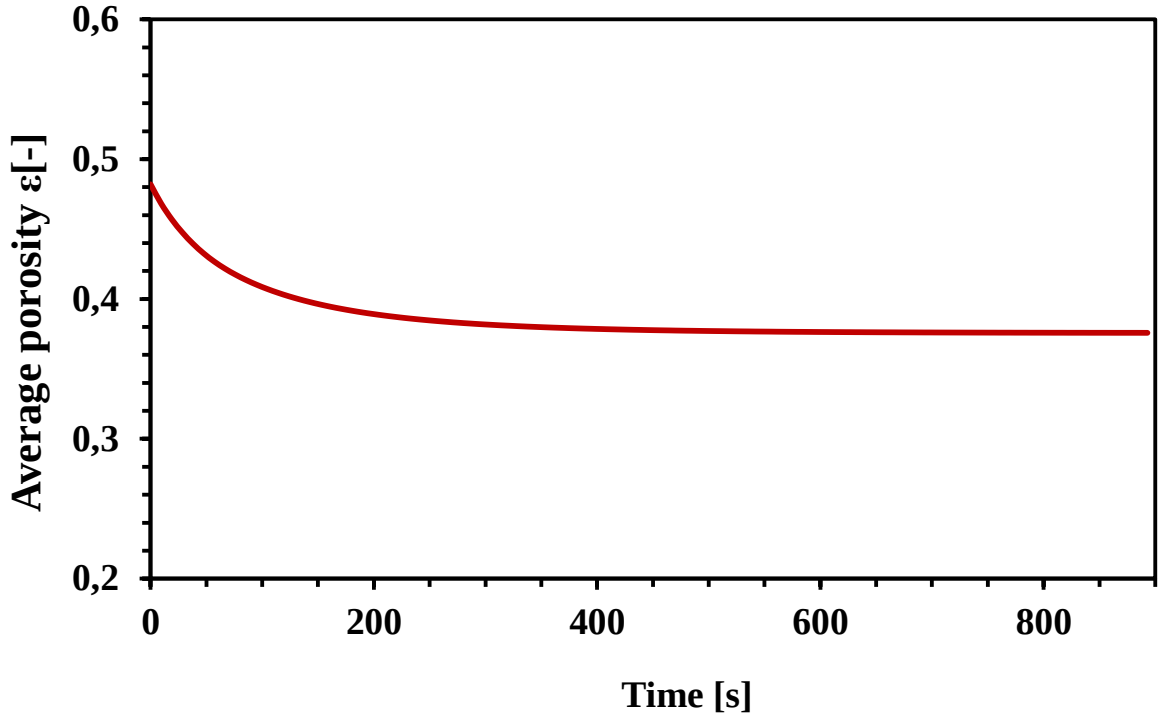

Figure 28 - Volume averaged porosity change over time

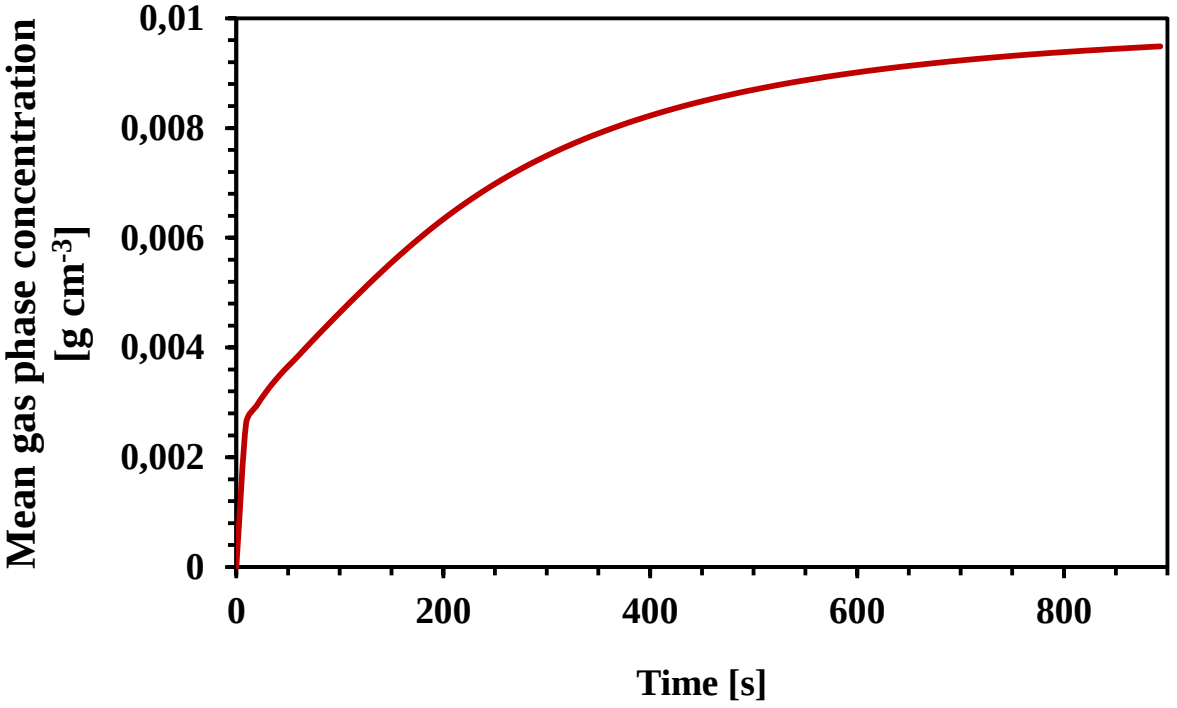

Figure 29 - Volume averaged mobile gas concentration over time

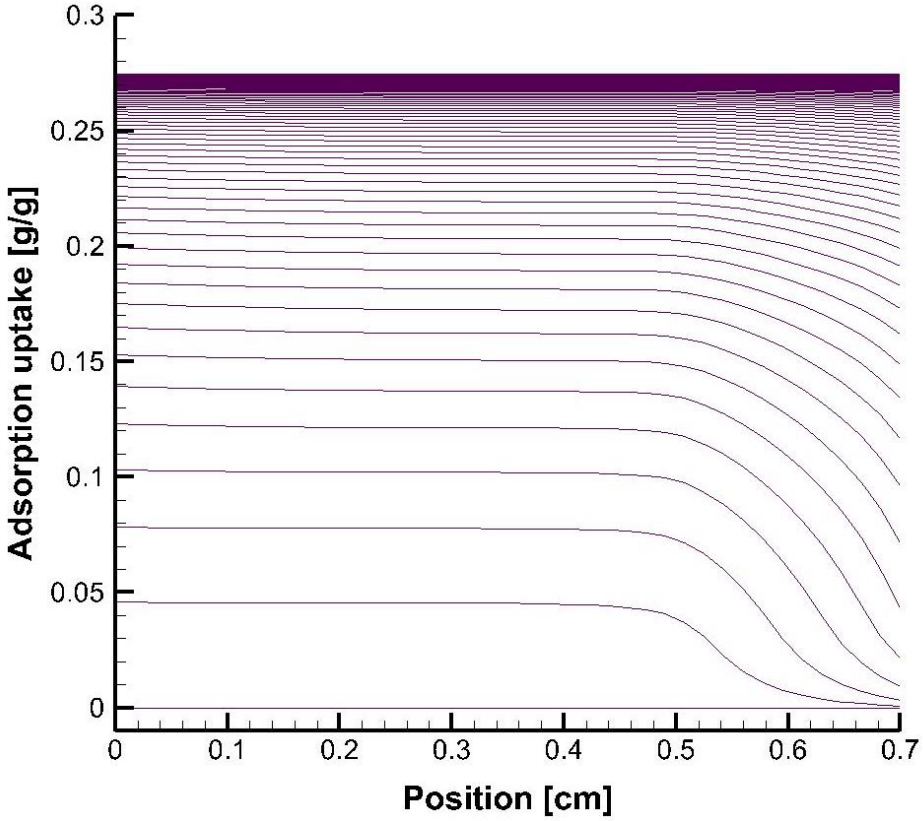

Figure 30 - Adsorption uptake

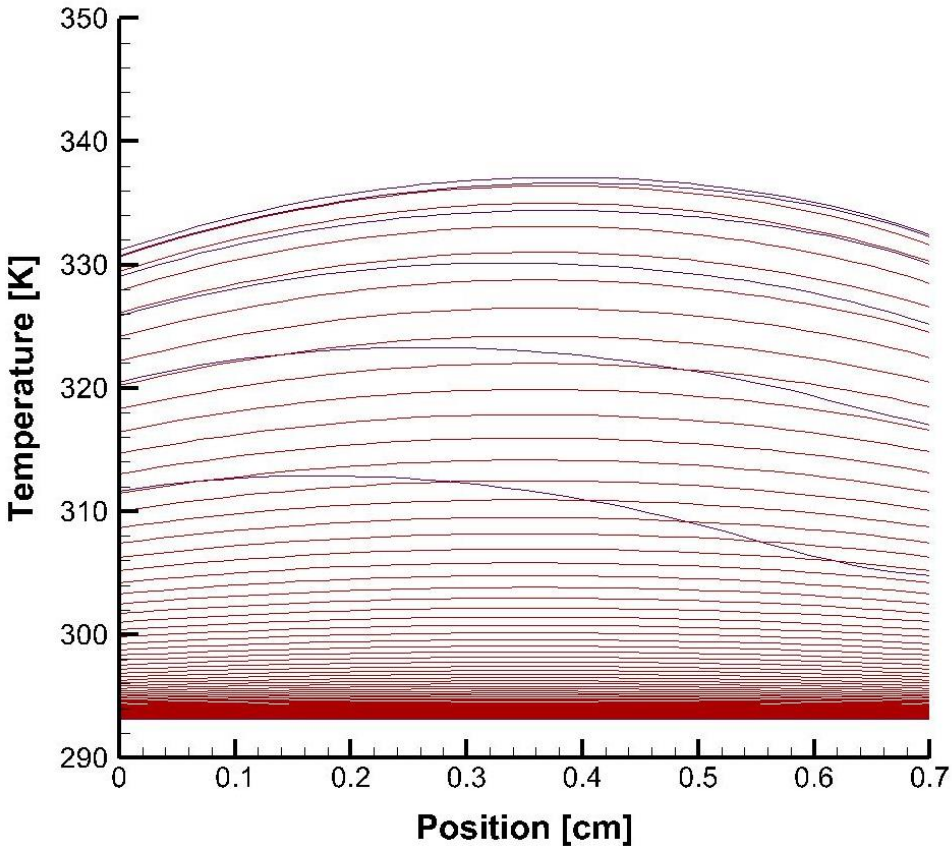

Figure 31 - Temperature distribution

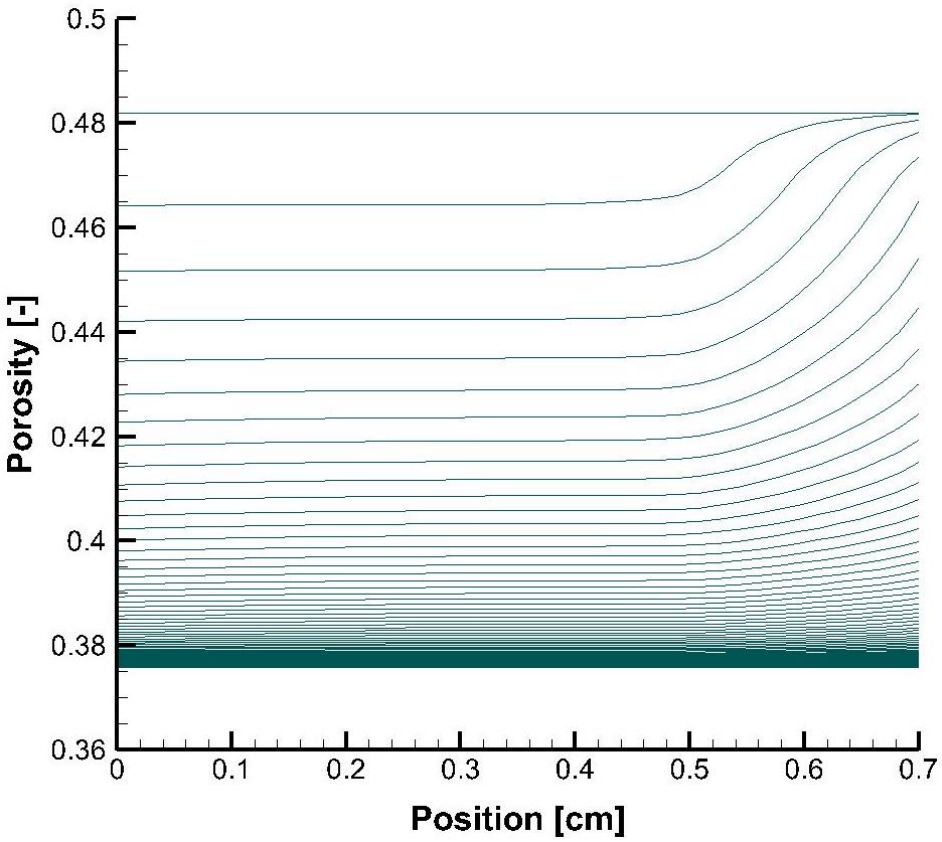

Figure 32 - Porosity change

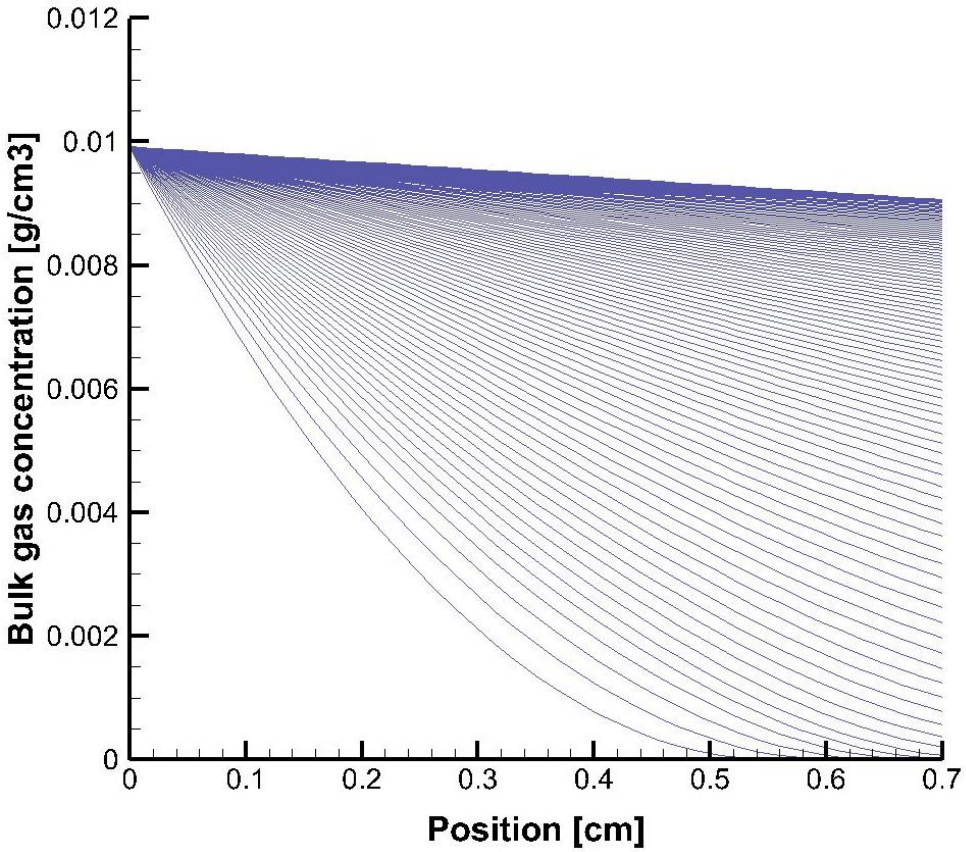

Figure 33 - Mobile gas concentration

CONCLUSION

The thesis is devoted to the study of the adsorption process and the adsorption characteristics of the material. The methods of analysis and post-processing of experimental data to establish the adsorption characteristics of the material are studied. An assessment of the adsorption and thermal characteristics of the newly synthesized material is performed. Analysis of the experimental data revealed 233% higher thermal conductivity than that for parent activated carbon. Composite showed specific BET surface area 1778 ± 13 m^2 g^{-1} and total pore volume 1.014 cm^3 g^{-1}. The consolidated composite adsorbent demonstrates improved volumetric adsorption uptake too. Magnetic suspension adsorption measurement apparatus was employed to measure the adsorption characteristics of composite/CO_2 pair for temperatures from 20 to 70°C for the pressures up to 5 MPa: two isotherms from subcritical and four isotherms from supercritical regions. Absolute adsorption was estimated from excess adsorption in two steps: firstly the absolute uptake was estimated using two different assumptions, after the average of above two methods was taken for avoiding these extreme assumptions and used in further analysis.

Obtained data were fitted to modified Dubinin-Astakhov (D-A) and Tóth isotherm models; thereby generalized isotherm models were constructed. Correlation errors for modified D-A and Tóth models in terms of the RMSD were 0.62% and 0.56%, respectively, which indicates a good approximation of data points. From the Tóth equation, the value of the isosteric heat of adsorption Q can be found during correlation stage, as the equation includes the isosteric heat of adsorption as a fitting parameter. When calculating the isosteric heat of adsorption from modified D-A model, it is found as a function of surface coverage. The average $\langle Q \rangle$ estimated using modified D-A and Tóth model were 19.742 kJ mol^{-1} and 19.023 kJ mol^{-1}, respectively [63, P. 131-140].

To calculate the adsorption uptake at the solid-gas interface, and for a detailed description of the dynamics of the adsorption process, a mathematical model of the non-isothermal reactive adsorption was constructed and solved. The mathematical model considers the adsorption caused porosity and Knudsen diffusivity changes. The temperature dependent adsorption rate change due to the energy release during adsorption process implemented through heat balance equation. The effective Knudsen diffusion coefficient for the working pair of CO_2/AC evaluated from Pore Size Distribution data. The experiment conducted on the magnetic suspension balance unit (MSB-GS-100-10 M) to measure the CO_2 adsorption onto composite activated carbon was simulated. The result obtained was compared with the results found using non-reactive isothermal model. Isothermal model includes only the material balance equations for the adsorbed and mobile phases. The model assumes the void fraction available for the gas phase to be constant. It simplifies the model and is reasonable since for the particular case under consideration $p_{eq} = 535\ kPa$, $T = 20°\ \mathrm{C}$ the volume of the adsorbed phase after saturation is around 15% of the pore volume. Non-isothermal reactive flow model gives more realistic curve shape of

volume averaged uptake with sharp increase in the adsorption starting and lower rate of mass uptake due to the release of the heat of adsorption. The rate gradually increases with time as the thermal energy dissipates to the surrounding through natural convection.

The model is numerically implemented in the Python using explicit difference schemes. The initial and boundary conditions are specified according to the features of the system under consideration. The curves of the concentration of the absorbed substance, the concentration of the mobile phase, the temperature and porosity fields are obtained as a function of time and coordinates. A comparative analysis of the existing and developed mathematical models is made. The solution method and the resulting dependency curves are appropriate. The validity and reliability of the scientific conclusions obtained in the thesis are confirmed by their consistent theoretical and mathematical justification, and a comparative analysis of the obtained simulation results with the experimental results is made.

The results of the presented dissertation are of great theoretical significance, and can be used for a detailed description of the dynamics of adsorption of carbon dioxide onto consolidated activated carbon. The developed mathematical model predicts the adsorption dynamics with better accuracy that isothermal non-reactive model. Residual deviations/errors in the results are associated with the use of 1D model geometry that excludes the gas penetration by the sides of the tablet. It's recommended to expand the model to 2D axial symmetry geometry for further research. The recommendation doesn't affect the main theoretical and practical results of the dissertation.

Work also has great practical significance, since the material has a direct purpose and is designed to improve and compact the adsorption refrigeration reactors. The enhancement of adsorption characteristics of the working pair in ACS has a positive impact on its performance. The composite showed promising CO_2 adsorption capacity and thermal characteristics which leads to development of compact CO_2 based adsorption cooling systems [98-100]. The development of this direction has great potential, since adsorption refrigerators operate on solar energy or waste heat, and can operate off-grid. Later the results obtained will be used in development of the fully solar driven ACS prototype. Such technology could be used in production of from small thermostats till huge storehouses with regulated temperature.

Novelty:

- new consolidated composite adsorbent with improved thermal conductivity and volumetric adsorption uptake was synthesized and the adsorption characteristics of the material studied comprehensively. Analysis of the experimental data revealed 233% higher thermal conductivity than that for parent activated carbon;
- absolute uptake was estimated from excess adsorption using two different methods. In the first method the specific volume of gas in the adsorbed state is assumed to be equal to the specific pore volume. In the other method the volume of adsorbed gas tends to zero under low pressure and/or high temperature conditions. The average was taken as the best closest fit. Obtained absolute adsorption data was

fitted to Dubinin-Astakhov and Tóth isotherm models. Correlation errors RMSD for modified D-A and Tóth models were 0.62% and 0.56% respectively;

- new mathematical model considering the adsorption caused porosity and Knudsen diffusivity changes was developed. The temperature dependent adsorption rate change due to the energy release during adsorption process is also implemented in the model. The effective Knudsen diffusion coefficient for the working pair of CO_2/AC evaluated from Pore Size Distribution data. The experiment conducted on the magnetic suspension balance unit (MSB-GS-100-10 M) to measure the CO_2 adsorption onto consolidated composite activated carbon was simulated.

The results are original, as they were carried out on new material, using more accurate methods for analysis. The first and second results were carried out in collaboration with a group of a foreign scientific adviser and are part of a scientific internship to Japan, on the results of which a joint paper was published in a journal.

The third result includes a number of novelties: the effective Knudsen diffusion coefficient for the working pair of carbon dioxide / activated carbon was found using the curve of the distribution of pores in size and on the characteristics of the diffused gas; the developed new mathematical model takes into account changes in porosity and Knudsen diffusion coefficient caused by adsorption uptake; the model also implements a temperature-dependent change in the rate of adsorption due to the heat of absorption; an experiment conducted on the equipment MSB-GS-100-10M for measuring the adsorption of carbon dioxide on a consolidated composite activated carbon was simulated.

REFERENCES

1 Singh, V.K., Kumar, E.A. Measurement of CO2 adsorption kinetics on activated carbons suitable for gas storage systems // Greenh. Gases Sci. Technol. - 2017. – Vol. 7, - P. 182–201. https://doi.org/10.1002/ghg.1641

2 Zakaria, Z., George, T. The Performance of Commercial Activated Carbon Absorbent for Adsorbed Natural Gas Storage // Int. J. Res. Rev. Appl. Sci. - 2011. - Vol. 9, - No. 2, - P. 225–230.

3 Sahoo, S., Ramgopal, M. Experimental studies on an indigenous coconut shell based activated carbon suitable for natural gas storage // Sādhanā. - 2016. – Vol. 41, - P. 459–468. https://doi.org/10.1007/s12046-016-0483-x

4 Ybyraiymkul, D., Ng, K. C., Kaltayev, A. Experimental and numerical study of effect of thermal management on storage capacity of the adsorbed natural gas vessel // Applied Thermal Engineering, - 2017. – Vol. 125. - P. 523–531. doi:10.1016/j.applthermaleng.2017.06.147

5 Fan, W., Chakraborty, A., Kayal, S. Adsorption cooling cycles: Insights into carbon dioxide adsorption on activated carbons // Energy. - 2016. Elsevier Ltd. https://doi.org/10.1016/j.energy.2016.02.112

6 Jribi, S., Saha, B.B., Koyama, S., Bentaher, H. Modeling and simulation of an activated carbon-CO2 four bed based adsorption cooling system // Energy Convers. Manag. - 2014. – Vol. 78. - P. 985–991. https://doi.org/10.1016/j.enconman.2013.06.061

7 Lemmini, F., Errougani, A. Building and experimentation of a solar powered adsorption refrigerator // Renew. Energy. - 2005. - Vol. 30, - No. 13, - P. 1989–2003. https://doi.org/10.1016/j.renene.2005.03.003

8 Pal, A., El-Sharkawy, I.I., Saha, B.B., Jribi, S., Miyazaki, T., Koyama, S. Experimental investigation of CO2 adsorption onto a carbon based consolidated composite adsorbent for adsorption cooling application // Appl. Therm. Eng. - 2016. - Vol. 109, -P. 304–311. https://doi.org/10.1016/j.applthermaleng.2016.08.031

9 Jribi, S., Chakraborty, A., El-Sharkawy, I.I., Saha, B.B., Koyama, S. Thermodynamic Analysis of Activated Carbon-CO2 based Adsorption Cooling Cycles // World Acad. Sci. Eng. Technol. - 2008. - Vol. 2, - No. 7, -P. 63–66.

10 Stritih, U., Bombač, A. Description and Analysis of Adsorption Heat Storage Device // Strojniški Vestn. – J. Mech. Eng., - 2014. - Vol. 60. - No. 10. - P. 619–628.

11 Lefebvre, D., Tezel, F.H. A review of energy storage technologies with a focus on adsorption thermal energy storage processes for heating applications // Renew. Sustain. Energy Rev. - 2017. - Vol. 67, - P. 116–125.

12 Chahbani, M.H., Labidi, J., Paris, J. Modeling of adsorption heat pumps with heat regeneration // Appl. Therm. Eng. - 2004. – Vol. 24, - P. 431–447. https://doi.org/10.1016/j.applthermaleng.2003.08.012

13 Meunier, F. Solid sorption heat powered cycles for cooling and heat pumping applications // Appl. Therm. Eng. - 1998. - Vol. 18, -P. 715–729.

14 Rezaei, F., Webley, P. Structured adsorbents in gas separation processes // Sep. Purif. Technol. - 2010. - Vol. 70, - P. 243–256. https://doi.org/10.1016/j.seppur.2009.10.004

15 Saxena, R., Singh, V.K., Kumar, E.A. Carbon dioxide capture and sequestration by adsorption on activated carbon // Energy Procedia, - 2014. – Vol. 54, - P. 320–329. https://doi.org/10.1016/j.egypro.2014.07.275

16 Singh, V.K., Kumar, E.A. Comparative Studies on CO2 Adsorption Kinetics by Solid Adsorbents // Energy Procedia, - 2015. – Vol. 90, - P. 316–325. https://doi.org/10.1016/j.egypro.2016.11.199

17 Dreisbach, F., Paschke, T. Gas Storage Capacity of MOF Materials - Measuring High Pressure Methane Adsorption // IsoSORP Application Note, - 2013. - No. 1, - P. 1–2.

18 Gwadera, M., Kupiec, K. Adsorption cooling as an effective method of waste heat utilization // Tech. Trans. -2011. - Vol. 108, - No. 8, - P. 61–70.

19 Kadam, Y.H., Yadav, D.H., Mohite, S.J., Panchal, P.P., Dongare, V.K. Design of Waste Heat Driven Vapour Adsorption Cooling System for Vehicle Air-Conditioning and Refrigeration // International Journal of Research in Engineering and Technology, - 2016. – Vol. 5. - P. 89–93.

20 Sakoda, A., Suzuki, M. Fundamental study on solar powered adsorption cooling system // Journal of Chemical Engineering of Japan, - 1984. –Vol. 17(1), - P. 52–57. doi:10.1252/jcej.17.52

21 Sumathy, K., & Zhongfu, L. Experiments with solar-powered adsorption ice-maker // Renewable Energy, - 1999. – Vol. 16(1-4), - P. 704–707. doi:10.1016/s0960-1481(98)00256-0

22 Askalany, A. A., Salem, M., Ismael, I. M., Ali, A. H. H., Morsy, M. G., Saha, B. B. An overview on adsorption pairs for cooling //Renewable and Sustainable Energy Reviews, - 2013. – Vol. 19, - P. 565–572. doi:10.1016/j.rser.2012.11.037

23 Habib, K., Saha, B. B., Koyama, S. Study of various adsorbent–refrigerant pairs for the application of solar driven adsorption cooling in tropical climates // Applied Thermal Engineering, - 2014. – Vol. 72(2), -P. 266–274. doi:10.1016/j.applthermaleng.2014.05.102

24 Ugale, V.D., Pitale, A. D. A Review on Working Pair Used in Adsorption Cooling System // International Journal of Air-Conditioning and Refrigeration, -2015. – Vol. 23(02), 1530001. doi:10.1142/s2010132515300013

25 Hildbrand, C., Dind, Ph., Pons, M., Buchter, F. A new solar powered adsorption refrigerator with high performance // Solar Energy, - 2004. – Vol. 77, - P. 311–318.

26 Hines, A., Kuo, S.-L., Dural, N. A New Analytical Isotherm Equation for Adsorption on Heterogeneous Adsorbents // Separation Science and Technology, - 1990. – Vol. 25(7), - P. 869–888. doi:10.1080/01496399008050371

27 Jribi, S., Miyazaki, T., Saha, B. B., Koyama, S., Maeda, S., Maruyama, T. Corrected adsorption rate model of activated carbon–ethanol pair by means of

CFD simulation // International Journal of Refrigeration, -2016. – Vol. 71, - P. 60–68. doi:10.1016/j.ijrefrig.2016.08.004

28 Anyanwu, E. E. Review of solid adsorption solar refrigerator I: an overview of the refrigeration cycle // Energy Conversion and Management, -2003. – Vol. 44(2), - P. 301–312. doi:10.1016/s0196-8904(02)00038-9

29 Askalany, A.A., Henninger, S.K., Ghazy, M., Saha, B.B. Effect of improving thermal conductivity of the adsorbent on performance of adsorption cooling system // Appl. Therm. Eng. - 2017. – Vol. 110, - P. 695–702. https://doi.org/10.1016/j.applthermaleng.2016.08.075

30 Mauran, S., Prades, P., L'Haridon, F. Heat and mass transfer in consolidated reacting beds for thermochemical systems // Heat Recovery Systems and CHP, - 1993. – Vol. 13(4), - P. 315–319. doi:10.1016/0890-4332(93)90055-z

31 Anyanwu, E. E. Review of solid adsorption solar refrigeration II: An overview of the principles and theory //Energy Conversion and Management, - 2004. – Vol. 45(7-8), - P. 1279 -1295. doi:10.1016/j.enconman.2003.08.003

32 Anyanwu, E. E., Ezekwe, C. I. Design, construction and test run of a solid adsorption solar refrigerator using activated carbon/methanol, as adsorbent/adsorbate pair // Energy Conversion and Management, - 2003. – Vol. 44(18), - P. 2879–2892. doi:10.1016/s0196-8904(03)00072-4

33 Miyazaki, T., Baran Saha, B., Koyama, S. Analytical Model of a Combined Adsorption Cooling and Mechanical Vapor Compression Refrigeration System // Heat Transfer Engineering, - 2016. – Vol. 38(4), - P. 423–430. doi:10.1080/01457632.2016.1195135

34 Zhao, Y. Study of Activated Carbon/Methanol Adsorption Refrigeration Tube and system Integration // Thesis submitted in fulfillment of the requirement for the degree of Master of Engineering Science, University of Adelaide. -2011.

35 Saha, B. B., Koyama, S., Kashiwagi, T., Akisawa, A., Ng, K. C., Chua, H. T. Waste heat driven dual-mode, multi-stage, multi-bed regenerative adsorption system // International Journal of Refrigeration, - 2003. – Vol. 26(7), - P. 749 – 757. doi:10.1016/s0140-7007(03)00074-4

36 Cherrad, N., Benchabane, A., Sedira, L., Rouag, A. Transient numerical model for predicting operating temperatures of solar adsorption refrigeration cycle // Applied Thermal Engineering, - 2018. – Vol. 130, - P. 1163–1174. doi:10.1016/j.applthermaleng.2017.11.059

37 Shen, C., Grande, C.A., Li, P., Yu, J., Rodrigues, A.E. Adsorption equilibria and kinetics of CO2 and N2 on activated carbon beads // Chem. Eng. J. - 2010. – Vol. 160, - P. 398–407. https://doi.org/10.1016/j.cej.2009.12.005

38 Tóth, J. Adsorption: Theory, Modeling, and Analysis. - New York, Basel: Marcel Dekker Inc., 2002. - Vol. 107. - P. 220-259.

39 Jribi, S., Miyazaki, T., Saha, B.B., Pal, A., Younes, M.M., Koyama, S., Maalej, A. Equilibrium and kinetics of CO2 adsorption onto activated carbon // Int. J. Heat Mass Transf. - 2017. – Vol. 108, - P. 1941–1946. https://doi.org/10.1016/j.ijheatmasstransfer.2016.12.114

40 Myers, A.L., Monson, P.A. Physical adsorption of gases: The case for absolute adsorption as the basis for thermodynamic analysis // Adsorption, - 2014. – Vol. 20, - No. 4, - P. 591–622. https://doi.org/10.1007/s10450-014-9604-1

41 Brandani, S., Mangano, E., Sarkisov, L. Net, excess and absolute adsorption and adsorption of helium // Adsorption, - 2016. – Vol. 22. – P. 261–276 DOI 10.1007/s10450-016-9766-0

42 El-Sharkawy, I.I., Pal, A., Miyazaki, T., Saha, B.B., Koyama, S. A study on consolidated composite adsorbents for cooling application // Appl. Therm. Eng. - 2016. – Vol. 98, - P. 1214–1220. doi.org/10.1016/j.applthermaleng.2015.12.105

43 Jin, Z., Tian, B., Wang, L., Wang, R. Comparison on thermal conductivity and permeability of granular and consolidated activated carbon for refrigeration // Chinese J. Chem. Eng. - 2013. - Vol. 21, - No. 6, - P. 676–682. https://doi.org/10.1016/S1004-9541(13)60525-X

44 Pal, A., Uddin, K., Thu, K., Saha, B.B. Activated carbon and graphene nanoplatelets based novel composite for performance enhancement of adsorption cooling cycle // Energy Convers. Manag. - 2019. – Vol. 180, - P. 134–148. https://doi.org/10.1016/j.enconman.2018.10.092

45 Wang, L.W., Tamainot-Telto, Z., Thorpe, R., Critoph, R.E., Metcalf, S.J., Wang, R.Z. Study of thermal conductivity, permeability, and adsorption performance of consolidated composite activated carbon adsorbent for refrigeration // Renew. Energy, - 2011. – Vol. 36, - No. 8, -P. 2062–2066. https://doi.org/10.1016/j.renene.2011.01.005

46 Rashidi, N. A., Yusup, S., Hameed, B. H. Kinetic studies on carbon dioxide capture using lignocellulosic based activated carbon // Energy, - 2013. – Vol. 61, - P. 440–446. doi:10.1016/j.energy.2013.08.050

47 Balsamo, M., Budinova, T., Erto, A., Lancia, A., Petrova, B., Petrov, N., & Tsyntsarski, B. CO2 adsorption onto synthetic activated carbon: Kinetic, thermodynamic and regeneration studies // Separation and Purification Technology, - 2013. – Vol. 116, - P. 214–221.doi:10.1016/j.seppur.2013.05.041

48 Ahn, H., Brandani, S. Dynamics of Carbon Dioxide Breakthrough in a Carbon Monolith Over a Wide Concentration Range // Adsorption, - (2005). – Vol. 11(S1), - P. 473–477. doi:10.1007/s10450-005-5970-z

49 Ribeiro, R. P., Sauer, T. P., Lopes, F. V., Moreira, R. F., Grande, C. A., Rodrigues, A. E. Adsorption of CO2, CH4, and N2in Activated Carbon Honeycomb Monolith // Journal of Chemical & Engineering Data, - 2008. – Vol. 53(10), - P. 2311–2317. doi:10.1021/je800161m

50 Li, S., Deng, S., Zhao, L., Zhao, R., Lin, M., Du, Y., Lian, Y. Mathematical modeling and numerical investigation of carbon capture by adsorption: Literature review and case study // Applied Energy, - 2018. – Vol. 221, - P. 437–449. doi:10.1016/j.apenergy.2018.03.093

51 Mulgundmath, V. P., Jones, R. A., Tezel, F. H., Thibault, J. Fixed bed adsorption for the removal of carbon dioxide from nitrogen: Breakthrough behaviour

and modelling for heat and mass transfer // Separation and Purification Technology, - 2012. – Vol. 85, - P. 17–27. doi:10.1016/j.seppur.2011.07.038

52 Farooq, S., Ruthven, D. M. Heat effects in adsorption column dynamics. 2. Experimental validation of the one-dimensional model // Industrial & Engineering Chemistry Research, - 1990. – Vol. 29(6), - P. 1084–1090. doi:10.1021/ie00102a020

53 Khalighi, M., Farooq, S., Karimi, I. A. Nonisothermal Pore Diffusion Model for a Kinetically Controlled Pressure Swing Adsorption Process // Industrial & Engineering Chemistry Research, - 2012. – Vol. 51(32), - P. 10659–10670. doi:10.1021/ie3004539

54 Pal, A., Shahrom, M.S.R., Moniruzzaman, M., Wilfred, C.D., Mitra, S., Thu, K., Saha, B.B. Ionic liquid as a new binder for activated carbon based consolidated composite adsorbents // Chem. Eng. J. - 2017. – Vol. 326, - P. 980–986. https://doi.org/10.1016/j.cej.2017.06.031

55 Pal, A., El-Sharkawy, I.I., Miyazaki, T., Saha, B.B. Adsorption Characteristics of Consolidated Adsorbents + Ethanol Pairs // in: 8th Asian Conference on Refrigeration and Air-Conditioning. - 2016. P. 8–11.

56 Pal, A., El-Sharkawy, I.I., Saha, B.B., Habib, K., Miyazaki, T., Koyama, S. Thermodynamic analysis of adsorption cooling cycle using consolidated composite adsorbents - ethanol pairs // ARPN J. Eng. Appl. Sci. - 2016. – Vol. 11, - P. 12234–12238.

57 Horváth, G., Kawazoe, K. Method for the calculation of effective pore size distribution in molecular sieve carbon // Journal of Chemical Engineering of Japan, - 1983. – Vol. 16. – No. 6. – P. 470-475. DOI:10.1252/jcej.16.470

58 Landers, J., Gor, G. Y., Neimark, A. V. Density functional theory methods for characterization of porous materials // Colloids and Surfaces A: Physicochemical and Engineering Aspects, - 2013. – Vol. 437, - P. 3–32. doi:10.1016/j.colsurfa.2013.01.007

59 Rocky, K.A., Amirul Islam, M., Pal, A., Ghosh, S., Thu, K., Nasruddin, Baran Saha, B. Experimental investigation of the specific heat capacity of parent materials and composite adsorbents for adsorption heat pumps // Applied Thermal Engineering, - 2020. – Vol. 164. 114431. doi:10.1016/j.applthermaleng.2019.114431

60 Zhou, L., Bai, S., Su, W., Yang, J., Zhou, Y. Comparative study of the excess versus absolute adsorption of CO2 on superactivated carbon for the near-critical region // Langmuir, - 2003. – Vol. 19, - No. 7, - P. 2683–2690. https://doi.org/10.1021/la020682z

61 Zhou, L., Zhou, Y. A Comprehensive Model for the Adsorption of Supercritical Hydrogen on Activated Carbon. Industrial & Engineering Chemistry Research, - 1996. – Vol. 35(11), - P. 4166–4168. doi:10.1021/ie960275g

62 Zhou, L., Zhou, Y. Linearization of adsorption isotherms for high-pressure applications // Chem. Eng. Sci. - 1998. - Vol. 53, - No. 14, - P. 2531–2536. doi.org/10.1016/S0009-2509(98)00065-7

63 Berdenova, B., Pal, A., Muttakin, M., Mitra, S., Thu, K., Saha, B. B., Kaltayev, A. A comprehensive study to evaluate absolute uptake of carbon dioxide

adsorption onto composite adsorbent // International Journal of Refrigeration, - 2019. Volume 100, Pages 131-140, doi:10.1016/j.ijrefrig.2019.01.014

64 Foo, K. Y., Hameed, B. H. Insights into the modeling of adsorption isotherm systems // Chemical Engineering Journal, - 2010. – Vol. 156(1), - P. 2–10. doi:10.1016/j.cej.2009.09.013

65 Rahman, M.M.; Muttakin, M.; Pal, A.; Shafiullah, A.Z.; Saha, B.B. A Statistical Approach to Determine Optimal Models for IUPAC-Classified Adsorption Isotherms // Energies, - 2019. – Vol. 12, 4565. doi:10.3390/en12234565

66 Singh, V.K., Anil Kumar, E. Measurement and analysis of adsorption isotherms of CO2 on activated carbon // Appl. Therm. Eng. - 2016. - Vol. 97, - P. 77–86. https://doi.org/10.1016/j.applthermaleng.2015.10.052

67 Amankwah, K.A.G., Schwarz, J.A. A modified approach for estimating pseudo-vapor pressures in the application of the Dubinin-Astakhov equation // Carbon, - 1995. - Vol. 33(9), - P. 1313–1319. doi:10.1016/0008-6223(95)00079-s

68 Б.Берденова, Е.Максум, Регрессионный анализ для определения параметров моделей изотерм адсорбции // Вестник КазНИТУ. - 2018. - № 4. - P. 233-240.

69 Srinivasan, K., Saha, B. B., Ng, K. C., Dutta, P., Prasad, M. A method for the calculation of the adsorbed phase volume and pseudo-saturation pressure from adsorption isotherm data on activated carbon // Physical Chemistry Chemical Physics, - 2011. – Vol. 13(27), - P. 12559. doi:10.1039/c1cp20383e

70 Rahman, K.A., Loh, W.S., Ng, K.C. Heat of adsorption and adsorbed phase specific heat capacity of methane/activated carbon system // Procedia Eng. - 2013. – Vol. 56, - P. 118–125. https://doi.org/10.1016/j.proeng.2013.03.097

71 Shen, D.,Bülow, M., Siperstein, F., Engelhard, M., Myers, A.L. Comparison of Experimental Techniques for Measuring Isosteric Heat of Adsorption // Adsorption, - 2000. – Vol. 6(4), - P. 275–286. doi:10.1023/a:1026551213604

72 Askalany, A.A., Saha, B.B. Derivation of isosteric heat of adsorption for non-ideal gases // International Journal of Heat and Mass Transfer, -2015. – Vol. 89, - P. 186–192. doi:10.1016/j.ijheatmasstransfer.2015.05.018

73 Azahar, F. H. M., Mitra, S., Yabushita, A., Harata, A., Saha, B. B., Thu, K. Improved model for the isosteric heat of adsorption and impacts on the performance of heat pump cycles // Applied Thermal Engineering, - (2018). – Vol. 143, - P. 688–700. doi:10.1016/j.applthermaleng.2018.07.131

74 Saha, B.B., Jribi, S., Koyama, S., El-sharkawy, I.I. Carbon Dioxide Adsorption Isotherms on Activated Carbons // J. Chem. Eng. Data, - 2011. - Vol. 56, - P. 1974–1981. https://doi.org/10.1021/je100973t

75 Himeno, S., Komatsu, T., Fujita, S. High-Pressure Adsorption Equilibria of Methane and Carbon Dioxide on Several Activated Carbons // J. Chem. Eng. Data, - 2005. - Vol. 50, - P. 369–376. https://doi.org/10.1021/je049786x

76 Singh, V.K., Kumar, E.A. Experimental investigation and thermodynamic analysis of CO2 adsorption on activated carbons for cooling system // J. CO2 Util. - 2017. - Vol. 17, - P. 290–304. doi.org/10.1016/j.jcou.2016.12.004

77 Singh, V.K., Kumar, E.A., Saha, B.B. Adsorption isotherms, kinetics and thermodynamic simulation of CO2-CSAC pair for cooling application // Energy, - 2018. - Vol. 160, - P. 1158–1173. https://doi.org/10.1016/J.ENERGY.2018.07.063

78 Singh, V.K., Kumar, E.A. Thermodynamic analysis of single-stage and single-effect two-stage adsorption cooling cycles using indigenous coconut shell based activated carbon-CO2 pair // Int. J. Refrig. - 2017. - Vol. 84, - P. 238–252. https://doi.org/10.1016/j.ijrefrig.2017.08.007

79 Dantas, T. L. P., Amorim, S. M., Luna, F. M. T., Silva, I. J., de Azevedo, D. C. S., Rodrigues, A. E., Moreira, R. F. P. M. Adsorption of Carbon Dioxide onto Activated Carbon and Nitrogen-Enriched Activated Carbon: Surface Changes, Equilibrium, and Modeling of Fixed-Bed Adsorption // Separation Science and Technology, - 2009. - Vol. 45(1), - P. 73–84.doi:10.1080/01496390903401762

80 Mugge, J., Bosch, H., Reith, T. Gas Adsorption Kinetics In Activated Carbon // Adsorption Science and Technology. - 2000. – P. 451-455. doi:10.1142/9789812793331_0090

81 Mohammad, N. K., Ghaemi, A., Tahvildari, K. Hydroxide modified activated alumina as an adsorbent for CO2 adsorption: Experimental and modeling // International Journal of Greenhouse Gas Control, - 2019. - Vol. 88, - P. 24–37. doi:10.1016/j.ijggc.2019.05.029

82 Rupa, M. J., Pal, A., Saha, B. B. Activated carbon-graphene nanoplatelets based green cooling system: Adsorption kinetics, heat of adsorption, and thermodynamic performance // Energy, - 2019. 116774. doi:10.1016/j.energy.2019.116774

83 Glueckauf, E. Theory of chromatography. Part 10.—Formulæ for diffusion into spheres and their application to chromatography // Trans. Faraday Soc. - 1955. - Vol. 51(0), - P. 1540–1551. doi:10.1039/tf9555101540

84 El-Sharkawy, I. I. On the linear driving force approximation for adsorption cooling applications // International Journal of Refrigeration, - 2011. - Vol. 34(3), - P. 667–673. doi:10.1016/j.ijrefrig.2010.12.006

85 Buzanowski, M. A., Yang, R. T. Extended linear driving-force approximation for intraparticle diffusion rate including short times // Chemical Engineering Science, - 1989. – Vol. 44(11), - P. 2683–2689. doi:10.1016/0009-2509(89)85211-x

86 Abouelella, D.M., Fateen, S.-E.K., Fouad, M.M. K. Multiscale Modeling Study of the Adsorption of CO2 Using Different Capture Materials // Evergreen. – 2018. – Vol. 5, - P. 43-51. https://doi.org/10.5109/1929729

87 Берденова Б. Математическая модель процесса докритической изотермической адсорбции CO2 на активированный уголь // Вестник КазНИТУ. – 2019. – № 6, - С. 751-756.

88 Ahmadpour, A., Diffusion and adsorption in porous media. http://ahmadpour.profcms.um.ac.ir/imagesm/282/stories/phocagallery/10-diffusion.pdf. 06.07.2018.

89 Okhovat, A., Ahmadpour, A., Ahmadpour, F., Yadegar, Z.K. Pore Size Distribution Analysis of Coal-Based Activated Carbons: Investigating the Effects of Activating Agent and Chemical Ratio // ISRN Chemical Engineering. - 2012. - Vol. 2012. Article ID 352574. 10 pages. doi.org/10.5402/2012/352574.

90 Pisani, L. Simple Expression for the Tortuosity of Porous Media // Transp. Porous. Med. - 2011. - Vol. 88, - P 193-203. https://doi.org/10.1007/s11242-011-9734-9

91 Changjae Kim, Hochang Jang, Jeonghwan Lee, Experimental investigation on the characteristics of gas diffusion in shale gas reservoir using porosity and permeability of nanopore scale // Journal of Petroleum Science and Engineering, - 2015. - Vol. 133. - P. 226-237. doi.org/10.1016/j.petrol.2015.06.008

92 Birkmann, F., Pasel, C., Luckas, M., Bathen, D. Trace Adsorption of Ethane, Propane, and n-Butane on Microporous Activated Carbon and Zeolite 13X at Low Temperatures // Journal of Chemical & Engineering Data, - 2017. - Vol. 62(7), - P. 1973-1982, doi: 10.1021/acs.jced.6b01068

93 Hu, J., Liu, H. CO2Adsorption on Porous Materials: Experimental and Simulation Study // Advances in CO2 Conversion and Utilization, -2010. - P. 209–232. doi:10.1021/bk-2010-1056.ch014

94 Berdenova, B., Kaltayev, A. Review of adsorption and thermal characteristics of activated carbon and its application in ANG storage and ACS systems // Bulletin of the National Academy of Sciences of the Republic of Kazakhstan, - 2017, - Vol. 3, - P. 27-36.

95 Chadam, J., Peirce, A., Ortoleva, P. Stability of Reactive Flows in Porous Media: Coupled Porosity and Viscosity Changes // SIAM Journal on Applied Mathematics. - 1991. - Vol. 51(3), - P. 684–692. doi:10.1137/0151035

96 Aristov, Y. I. Adsorptive transformation of heat: Principles of construction of adsorbents database // Applied Thermal Engineering, - 2012. - Vol. 42, - P. 18–24. doi:10.1016/j.applthermaleng.2011.02.024

97 Chakraborty, A., Saha, B. B., Koyama, S., Ng, K. C. Specific heat capacity of a single component adsorbent-adsorbate system // Applied Physics Letters, - 2007. - Vol. 90(17), 171902. doi:10.1063/1.2731438

98 Берденова Б., Стационарные системы адсорбционного охлаждения работающие на экологически чистых хладагентах // тезис в материалах конференции, XIII Международная научная конференция студентов, магистрантов и молодых ученых «Ломоносов-2017 », г. Нур-Султан, - 2017, -С. 86-87.

99 Maksum Ye., Berdenova B. Analysis of the thermodynamics of adsorption cooling systems with the working pair of activated carbon/CO2 // thesis in conference proceeding, V International scientific conference of students and young scientists “Farabi alemi”, Almaty, - 2018, - P. 61.

100 Берденова Б., Сверхкритический цикл работы холодильного оборудования на углекислом газе // тезис в материалах конференции «Международные Фарабиевские чтения-2019» , Алматы, - 2019, - С. 64.